2022-10

HARMONIC MITIGATION IN OPTIMALLY SIZED AND LOCATED GRID CONNECTED SOLAR SYSTEM USING HYBRID POWER FILTER (CASE STUDY: BAHIR DAR DISTRIBUTION FEEDER R5-02)

MIERAF, DESALEGN FELEKE

BAHIR DAR UNIVERSITY

BAHIR DAR INSTITUTE OF TECHNOLOGY

SCHOOL OF RESEARCH AND POSTGRADUATE STUDIES

FACULTY OF ELECTRICAL AND COMPUTER ENGINEERING

POST GRADUATE PROGRAM IN POWER SYSTEM ENGINEERING

HARMONIC MITIGATION IN OPTIMALLY SIZED AND LOCATED GRID CONNECTED SOLAR SYSTEM USING HYBRID POWER FILTER (CASE STUDY: BAHIR DAR DISTRIBUTION FEEDER R5-02)

By:

MIERAF DESALEGN FELEKE

BAHIR DAR, ETHIOPIA

OCTOBER, 2022

i

BAHIR DAR UNIVERSITY
BAHIR DAR INSTITUTE OF TECHNOLOGY
FACULTY OF ELECTRICAL AND COMPUTER ENGINEERING

HARMONIC MITIGATION IN OPTIMALLY SIZED AND LOCATED GRID CONNECTED SOLAR SYSTEM USING HYBRID POWER FILTER (CASE STUDY: BAHIR DAR DISTRIBUTION FEEDER R5-02)

By:

Mieraf Desalegn Feleke

A thesis submitted to the school of Research and Graduate Studies of Bahir Dar Institute of Technology, Bahir Dar University, in partial fulfillment of the requirements for the award of the degree of **Master of Science in Power Systems** in Faculty of Electrical and Computer Engineering.
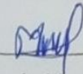
Advisor Name: Dr. Tassew Tadiwos

BAHIR DAR, ETHIOPIA

OCTOBER, 2022

BAHIR DAR UNIVERSITY

BAHIR DAR INSTITUTE OF TECHNOLOGY

SCHOOL OF RESEARCH AND GRADUATE STUDIES

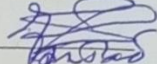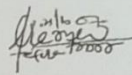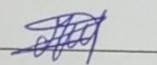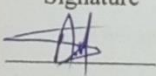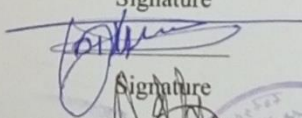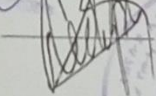**FACULTY OF ELECTRICAL AND COMPUTER ENGINEERING**

Thesis Approval Sheet

I hereby confirm that the changes required by the examiners have been carried out and incorporated in the final thesis.

Name of Student: - <u>Mieraf Desalegn</u> Feleke Signature _____ Date <u>18/10/2022G.C</u>

As members of the board of examiners, we examined this thesis entitled "Harmonic Mitigation in Optimally Sized and Located Grid Connected Solar System Using Hybrid Power Filter" by Mieraf Desalegn. We hereby certify that the thesis is accepted for fulfilling the requirements for the award of the degree of Masters of science in "Power System Engineering."

Board of Examiners

Name of Advisor	Signature	Date
<u>Dr. Tassew Tadiwos</u>		25/10/2022
Name of External examiner	Signature	Date
<u>Dr. Tefera T.</u>		21/10/2022
Name of Internal Examiner	Signature	Date
<u>Dr. Mezigebu G.</u>		05/10/2022
Name of Chairperson	Signature	Date
<u>Mr. Abriham H.</u>		31/10/2022
Name of Chair Holder	Signature	Date
<u>Mr. Yosef B.</u>		01/11/2022
Name of Faculty Dean	Signature	Date

Yaw Bewodros G. Workineh
Electrical and Computer
Engineering Faculty Dean

Mershu GC(Ph.D)
Pc coordinator

iii

iii
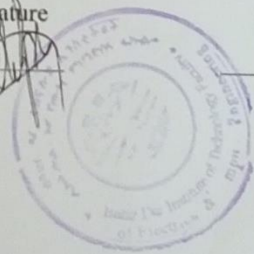
DECLARATION

This is to certify that the thesis entitled "Harmonic Mitigation in Optimally Sized and Located Grid Connected Solar System Using Hybrid Power Filter", submitted in partial fulfillment of the requirements for the degree of Master of Science in Power System Engineering under Electrical and Computer Engineering Faculty, Bahir Dar Institute of Technology, is a record of original work carried out by me and has never been submitted to this or any other institution to get any other degree or certificates. The assistance and help I received during the course of this investigation have been duly acknowledged.

Name of the student: Mieraf Desalegn   Signature _____
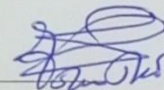
Date of submission: 18/10/2022
Place: Bahir Dar

This thesis has been submitted for examination with my approval as a university advisor

Advisor Name: Dr. Tassew Tadiwos   Signature: _____

iv

ACKNOWLEDGEMENT

ABSTRACT

Renewable energy plays a significant role in the power generation revolution in line with the future smart grid focus. one of the most abundant, clean and green energy productions is the solar energy. Bahir Dar distribution network is a type of radial distribution system, not only a substantial amount of power is lost but also the voltage profile of distant nodes from the main supplying substation are frequently below the acceptable limit especially during heavy load conditions. This in turn exposes the end consumers to continuously suffer from under-voltage problem. The voltage profiles of most of the buses in feeder R5-02 are not in the acceptable voltage level (i.e., 0.95-1. 05p.u interval). Moreover, the total real power loss of the feeder is 182.75 KW. The solar system is connected with the grid system to improve voltage profile and reduce power loss. The PSO (particle swarm optimization) algorithm is used to determine the optimal size and location of the solar system in the R5-02 Feeder. The minimum voltage is increased from 0.9378p.u to 0.9601p.u and the total real power loss is reduced 76.8 KW after connecting 2MW PV at bus 20. But an inverter which introduces harmonics into the grid is required to connect a photovoltaic system to the grid. Voltage and current waveforms lose their sinusoidal shape due to harmonics. According to the FFT (Fast Fourier transform) analysis, the inverter in grid-connected photovoltaic system has THD (total harmonic distortion) of 29.94%, which is higher than the IEEE standard of 5%. In this thesis, Hybrid Power Filter (shunt passive and shunt active filter) is simulated using MATLAB SIMULINK. The simulation result indicates that the THD of the system is reduced from 29.94% to 8.82% after connecting Shunt Passive filter only at the PCC (point of common coupling). The THD of the system is reduced from 29.94% to 4.55% after connecting Shunt active filter only. The THD of the system is reduced from 29.94% to 2.39% after connecting Hybrid power filter which is less than IEEE-519 standard of 5%. Compared to passive and shunt active power filters, hybrid power filter performs better and also reduce the kVA rating of Shunt active filter.

Keywords: **PV system, Particle Swarm Optimization, Power Loss, Voltage Profile, Total Harmonic Distortion, Active power filter, Hybrid power filter**

TABLE OF CONTENTS

LIST OF ACRONYMS

AC	Alternative current
APF	Active Power Filter
BCBV	Branch Current to Bus Voltage
BIBC	Bus Inject to Branch Current
DC	Direct Current
DG	Distributed Generation
EEP	Ethiopia electrical power
EMI	Electromagnetic Interference
GA	Genetic Algorithm
HPF	Hybrid Power Filter
IEEE	Institute of Electrical and Electronics Engineers
MATLAB	Matrix Laboratory
PCC	Point of common coupling
PPF	Passive Harmonic Filter
PSO	Particle swarm optimization
PV	Photovoltaic
SAPF	Shunt active power filter
THD	Total Harmonic Distortion
UPS	Uninterruptable power supply

LIST OF SYMBOLS

A	Ampere
Km	Kilo meter
Kv	Kilo volt
Kvar	Kilo var
Kw	Kilo watt
KWh	Kilo watt hour
LC	Inductor- Capacitor filter
LCL	Inductor- Capacitor-Inductor filter
m	Meter
Mvar	Mega var
MW	Mega watt
P	Active power
Q	Reactive power
V	Voltage
Vbase	System common voltage (base)

LIST OF FIGURES

xiv

LIST OF TABLES

CHAPTER ONE
INTRODUCTION

An electrical power system is an integrated network of generating stations, transmission lines and distribution systems for delivering electricity from generation to end users and operated by one or more control centers. Power is generated at the generation stations and delivered to end users through transmission and distribution systems. The distribution system is an essential component of power system which can deliver economical, reliable and quality power to end users. However, power system reliability is affected due to long service of infrastructures, demand-supply imbalance and radial type of network configuration. Radial type of configuration has high power loss which in turn affects the voltage profile of the system.

1.1 Background

The emphasis has turned to producing power from renewable energy sources including solar, wind, biomass, micro hydraulic, and tidal that do not release greenhouse gases as a result of the rise in electricity consumption and growing environmental concerns. The technologies used for renewable energy are growing quickly due to increasing energy demand, high cost of fuel, and environmental pollution and disturbances. The development of these technologies is important for the generation of effective energy with lower environmental pollution. However, integration of these energy resources will have negative impacts on system power flow and voltage based on the type of energy integrated, the network configuration and operating condition [1].

The photovoltaic system has become one of the most widely used renewable energy sources because, it is environmentally friendly, noiseless, low operating cost, high reliability in modules (>20 years), can be integrated into new or existing systems, and can be installed at nearly any point of use.

Integration of solar photovoltaic system with grid connection would assist in supplementing the continually increasing of electricity need in Ethiopia. Greater use of PV systems can also increase reliability of the electricity grid. Many problems exist arising from the operation of PV system jointly with the grid. It may lead to high power losses and

bad voltage profiles. For enhancing voltage support in distribution networks, it is very important to optimize the placement and size of such a system. So, when designing distribution systems, it is essential to consider the optimal placement and sizing of grid-connected PV. [2].

The integration of PV system in distribution system would lead to improving the voltage profile and reduce active power loss in Power supply. If the PV penetration is really high Photovoltaic systems might subject the grid to various negative affects. They are reverse power flow, overvoltage along distribution feeders, voltage control difficulty, power quality problems/ harmonics, increased reactive power and islanding detection difficulty [3]. If power quality problems caused by this interconnection are not properly handled, particularly harmonic problems, they could be exceedingly harmful to the grid and distribution system. A power electronics inverter is used to connect a PV system to the grid; this device injects harmonics into the grid.

There are two types of harmonics associated with renewable energy-based DG units. The first type of harmonics is generated by power electronic devices in renewable energy sources. For certain types of renewable energy sources such as PV systems, the grid connection is achieved through an interfacing power electronic inverter. The switching of power electronic devices in these inverters generates harmonics at DG`s output. For example, a PV inverter may experience high frequency switching during low irradiance level of solar energy, resulting in an injection of highly distorted current to the distribution network [1]. Such harmonics contain high frequency harmonic components at multiples of the carrier frequency of the inverter. To mitigate such harmonics, the grid-tie filters such as LCL (inductor-capacitor-inductor) or LC (inductor-capacitor) filters are used at the output of the inverters. These filters can potentially cause a harmonic resonance for system operation if not properly designed.

The harmonics need to be filtered out in order to retain the quality of the electricity delivered. In order to accomplish this, a device called Filter is used. IEEE standards have defined limits for harmonic voltages and currents. Low-voltage distribution systems can have up to 3.0% individual harmonics and 5.0% total harmonic distortion [4].

A passive filter is required to trap the harmonic current to correct the power factor of the load and properly filter the harmonics of the load. Traditional passive filtering approach is no longer attractive due to several shortcomings. Because the harmonics that need to be suppressed are often low order, the filter components are very bulky. Passive filters are known to cause resonance and hence affecting the stability of power system. It will not work effectively for varying load conditions [5].

An active power filter (APF) compensates for harmonics and corrects the power factor by supplying the harmonic currents drawn by non-linear loads. Generally, the active filter is connected in parallel with the harmonic-inducing load. Here PI control Technique is used for providing control signal. Sensed dc voltage of the APF is compared with its set reference value in the error detector, voltage error is processed in the Proportional-Integral (PI) controller according to that gating pulse are generated with pulse width modulation technique. APF has high performance but it requires high cost [5].

Hybrid connections of Active Filter and Passive Filter are also employed to reduce harmonics distortion levels in the network. The Passive Filter with fixed compensation characteristics is ineffective to filter the current harmonics. Active Filter overcomes the drawbacks of the Passive Filter by using the switching-mode power converter to perform the harmonic current elimination. The Active filter power rating of power converter is very large. Using low cost Passive Filter in the Hybrid power filter, the power rating of active converter is reduced compared with that of Active power filter. Hybrid power filter retains the advantages of Active filter and does not have the drawbacks of Passive filter and Active filter [6].

Passive filter and Active filter mitigation techniques have their own advantage and disadvantage. Particularly for high-power applications, the hybrid power filter is more desirable than the pure filters in terms of harmonic filtering from a viability and cost-savings perspective. In this thesis, the distribution system load flow analysis was done and analyze the distribution system with power loss and voltage profile issues using Backward Forward load flow analysis. The optimal location and size of solar system in the selected feeder is identified by PSO algorithm. The grid connected PV system without filter is modelled by MATLAB/SIMULINK. The individual and total harmonic distortion was

analyzed by FFT analysis. And design Hybrid Power Filters to mitigate the harmonic distortion. Finally compare harmonic distortion without filter, with passive filter, with active filter and with Hybrid power filter.

1.2 Statement of Problem

There is a continuous and gradual growth in the proportion of people living in Bahir Dar which in turn increases an electrical energy demand for residential customers and industrial companies. This leads to an installation of new additional distribution transformers on the existing radial distribution system very far from the substation especially in feeder R5-02. As a result, large voltage drop exists due to a high value of resistance to reactance ratio (R/X) of the distribution lines. There is also a significant power loss and the voltage profile of distant nodes from the main supplying substation are frequently below the minimum threshold value sometimes less than 0.93 p.u especially during heavy load conditions. Therefore, the distribution system performance is improved by optimally sizing and placing PV system using PSO algorithm.

If not properly managed, power quality problems resulting from the interconnection of PV system to the grid could be exceedingly harmful to the distribution system, especially harmonic problems. An inverter, which introduces harmonics into the grid, is required to connect a PV system to the grid. Harmonics results malfunctioning and failure of electrical equipment like transformers, cables and motors, excessive measurement errors in metering equipment and electromagnetic interference in high frequency communication systems such as television, radio, communication and telephone systems. Harmonics increase business operating costs by reducing system capacity, increase maintenance, increase replacement Costs of equipment failing prematurely. In this thesis, hybrid power filter is designed to reduce the harmonics produced by inverter.

1.3 Objectives of the Thesis

1.3.1   General Objective

The main objective of this thesis is to mitigate the harmonics of grid connected PV system and improving distribution system performance in a radial distribution system by determining the optimal location and size of PV system.

4

1.3.2 Specific Objective

- To model a radial distribution system and analyze voltage profile and power loss.
- To determine the optimal location and size of PV system in the Feeder R5-02.
- To conduct harmonic analysis without filter and compare the result with IEEE standard.
- To design a Hybrid power filters for mitigation of harmonic distortion and achieve low THD.

1.4 Scope

In this thesis work, the focus lays mitigation of harmonics of grid connected PV system which is case study on Bahir Dar distribution system radial feeder (feeder R5-02). The mitigation techniques are applied on the optimal sized and placed PV system which is done by using particle swarm optimization. Only the harmonic effect caused by the integration of PV system is considered. The analysis of harmonic distortion will be done on with and without filter. Then finally, this research work concludes with the result and recommendation up to giving future work direction. Only one feeder is considering in this thesis.

1.5 Significance of this Thesis

- To identify the main causes of interruption of the power system and point out solutions.
- Important to motivate both consumers and utilities to use solar energy.
- Help customers to reduce environmental pollution.
- Solves high power demand of end users and helps them to get quality power.
- Reduces cost of transmission and extra cost required due to power interruption.
- To ensure proper operation of equipment and a longer equipment life span by keeping values of harmonic distortion in acceptable limit on a distribution system.
- Power-loss reduction.

1.6 Thesis Organization

To make this work easy, the contents have been divided into six chapters. A brief overview of each chapter is given as follows.

Chapter One: Provides an introduction about impacts of PV system integration to the distribution system, distribution system power loss and voltage profile improvement, grid connected PV system and its negative impact, harmonics and its mitigation techniques. Problem statement, objectives, methodology, background of the study, scope and significance of the thesis are presented.

Chapter Two: Discusses literature reviews on distribution system performance enhancement methods, PV system allocation and sizing methods, harmonic mitigation techniques, control strategies of active power filter proposed by different researchers. Theoretical background of Photovoltaic system, load flow analysis of radial distribution network, Forward/backward sweep load flow method, and particle swarm optimization, harmonics and its source, effect and mitigation techniques are presented.

Chapter Three: Discusses the methodologies followed to conduct this thesis which comprises problem formulation, data collection, data analysis, optimal sizing and placement of PV system. Sizing of grid connected solar plant, Selection of PV panel, Boost converter and Inverter was done. Design of shunt passive and active filter for harmonic mitigation in grid connected PV system was done.

Chapter Four: Reveals the results obtained during the simulation and the discussion about the results found. Power loss and voltage profile of the system with and without PV system is clearly stated. The THD of grid current is compared without filter, with passive filter and with Hybrid filter.

Chapter Five: Discusses the conclusion for the results obtained during simulation and recommendation about future works.

CHAPTER TWO
LITERATURE REVIEW AND THEORETICAL BACKGROUND

2.1 LITERATURE REVIEW

Different kinds of literature are extensively discussed about different optimization algorithms that determine the optimal size and location of grid connected PV system and harmonic mitigation techniques on grid connected PV system.

2.1.1 Optimal size and location of grid connected PV system

[7] done on optimal placement and sizing of DG using PSO to improve the voltage profile of the distribution system with the objective function of improving voltage stability. DG units are connected in parallel with the utility grid, and they are placed depending on the availability of the resources. Integrating DG units can have an impact on the practices used in distribution systems, such as the voltage profile, power flow, power quality, stability, reliability, and protection. The proposed approach is simulated in MATLAB environment by testing on standard IEEE 33 bus and 69 bus distribution systems. This research addresses only voltage profile improvement. It did not address power loss minimization.

[8] Presents a Particle Swarm Optimization (PSO) based algorithm for optimal location of multiple PV DGs into the power distribution network for power loss minimization. The proposed algorithm has two major steps; first step is the finding of optimal location and active power injections of multiple PV DGs and later is the computation of optimal reactive power injection of PV DGs. The proposed method is successfully tested on IEEE 13 bus system and its performance has been benchmarked with the Improved Analytical method. The proposed technique effectively solved multiple PV DGs optimal location problem. Optimal locations and preferable active power injection of PV DGs are computed using PSO technique. Through the optimal location of multiple PV DGs in the power distribution network, network power losses are minimized and voltage profile is improved.

[2] Presents a new methodology using particle swarm optimization (PSO) for the placement of distributed generation (DG) in the radial distribution systems to reduce the power loss. Single PV DG placement is used to find the optimal DG location and its size which corresponding to the maximum loss reduction. The proposed method is tested on the

26-bus radial distribution system which modified from the Provincial Electricity Authority (PEA) distribution system. The load flow analysis on distribution use forward-backward sweep methodology. The simulation results show that PSO can obtain the maximum power loss reductions. In this paper, a particle swarm optimization for optimal placement of PV DG is efficiently minimizing the total real power loss satisfying transmission line limits and constraints. The methodology is fast and accurate in determining the sizes and locations.

2.1.2 Harmonic reduction in grid connected PV system and Nonlinear loads

[9] Presented a harmonic mitigation study in the standalone system, using three types of passive filters namely, series reactor and shunt passive filters such as single tuned and high pass filters in eliminating harmonics. Line reactor offers the advantage of his simplicity and low cost it provides no system resonance condition and it can achieve a significant reduction in harmonics but the total harmonic distortion cannot be below to 5% that is why use of shunt passive filters was necessary to improve system quality. However, passive filters have major weaknesses of bulky sizes and fixed mitigation abilities.

[10] Design LCL filter for reduction of harmonics in the three-phase PV grid-connected inverters. Firstly, analyze the inductance, the ration of two inductances, selecting the filter capacitor and resonance resistance. Based on these theories, a LCL filter is designed. The simulation result indicated that the LCL filter achieve the best performance than L filter and LC filter. Under the prerequisite of increasing system stability, parallel resistor is even more advantageous than series resistor. The simulation indicated that an LCL filter with a shunt damping resistor mitigated harmonics to 0.26%.

[11] Proposed Double-Tuned filter for mitigation of harmonic with relative to the test case grid condition. Double-Tuned filter, which is also categorized as Specific Harmonic Elimination (SHE) filter filters dominant harmonic at desired frequencies. A single tuned filter can only filter specific frequency harmonic and has several drawbacks such as larger component size, higher power losses and costing. The double tuned filters are the advancement of single tuned filters. It is designed to improve the performance of passive filters mainly single tuned filter as well as being much economical. However, the

capacitance of double tuned filter may cause a resonance problem if initial THD-I is less than 20% and it doesn't eliminate the tuned harmonics, but it only mitigates it.

[12] Design and analyze the passive LLCL filter for mitigation of the total harmonic distortion for current (THDI) in the proposed off grid PV system. The passive LLCL filter is practically installed between solar inverter and nonlinear load. This study describes a design methodology of a LLCL filter for off-grid power system with a comprehensive study of how to mitigate the harmonics in stand-alone solar system. The LLCL filter mitigates the THDI that injected by a six-pulse rectifier which is used as a non-linear load. The simulation result shows that the reduction of THDI from 89.89% to 3.257%. This paper attempts to show that the using of LLCL filter with a stand-alone solar system can highly improve the power quality of the system.

[13] Presents a three-phase voltage fed type shunt active filter system based on hysteresis current control to eliminate harmonic generation due to nonlinear loads towards a grid-connected PV system. The major limitation of these study is to limit the cost and the size of the inverter because APF has high performance but it requires high cost.

[14] This research work mainly focused on harmonic mitigations due to non-linear loads of a grid-connected PV system using a shunt active power filter. The three-phase voltage fed integrated shunt APF was developed based on hysteresis current control for harmonic elimination. The analysis and simulation results showed that the shunt APF system effectively damps out the harmonics effect from the nonlinear loads and reduces the THD level of the inverter current. It was demonstrated that the reference current from the shunt APF system keeps the inverter current to maintain its fundamental component and to avoid nonlinear load effect. The shunt APF works effectively to reduce additional harmonics. The THD of the inverter current was reduced from 21.51% to 2.51% which fits well IEEE standard.

[15] Presented a new control of grid interfacing inverter to improve the power quality. And the grid interfacing inverter can be effectively used for power conditioning without affecting real power transfer. The main goals of the proposed project are to enhance THD (Total Harmonic Distortion) and eliminate source current harmonics in grid-connected

hybrid renewable energy conversion systems. The VSC can thus be utilized as power converter to inject power generated from renewable energy source to the grid, and shunt APF to compensate current harmonics. To improve THD in grid connected hybrid system a fuzzy logic controller will be implemented to control VSC. The SAPF (shunt active power filter) has capability of injecting currents that is in sinusoidal with low THD, and also compensate problems like power factor, current harmonics and unbalance.

[16] Studies different control techniques for Shunt Active Power Filters. In this study, the synchronous reference frame theory, the instantaneous p-q approach, and the hysteresis current control of shunt active filters are investigated. MATLAB software was used to carry out the real implementation of p-q theory and synchronous reference frame theory in shunt active filters.

[17] Presented the simulation results for the proposed APF with Hysteresis Current Control (HCC) method. The used of HCC can reduce the switching losses in sinusoidal supply current signal and reduce the THD level to comply with IEEE 519 standard, thus, solve the power quality problems. It is strongly advised to use hysteresis current control techniques in industrial and home applications like three-phase induction motors in the future. The use of such method in three-phase induction motors can solve the distorted supply current waveform due to the non-linear torque, flux and current regulation. As a result, the power factor of the power supply system can be improved by lowering the THD level and switching losses. The planned HCC was validated with MATLAB in order to verify the proposed operation.

Each of the research works mentioned above have their own advantages and drawbacks of its own. However, this thesis work uses a suitable technique for selecting the optimal size and placement of PV system that is PSO algorithm to reduce electric power losses and improve voltage profile. Additionally, a hybrid power filter is used, which is the most practical and cost-effective method of harmonic issue reduction.

2.2 Photovoltaic Power System

Photovoltaic energy is the direct conversion of sunlight into electricity when light strikes the cell surface and release atoms and electrons of the semiconductor material. The

electrons are excited due to incoming light and moving through silicon material which leads to a flow of current. Electricity in the form of direct current (DC) is generated due to the photovoltaic effect when solar radiation hits the module. The electrical energy in DC form can be stored in a battery for off light hours or can be injected to the grid in alternating current (AC) form using an inverter for conversion [18].

The photovoltaic solar cells are made from semiconductor materials. PV cells are typically only a few inches in diameter, but the connection of multiple cells form a module. The connection of modules also forms an array. Then after a very large system can be formed by connecting arrays. PV module consists of many PV cells connected in parallel to increase current and in series to produce a higher voltage [19].

2.3 Advantages of the photovoltaic system

- ❖ Solar energy is supplied by nature thus it is abundant
- ❖ It can be made available almost anywhere there is sunlight
- ❖ Ease of operation and negligible operating cost
- ❖ Pollution free [20]
- ❖ Quick design, installation, and startup times for new plants.
- ❖ Power output matches very well with peak load demands.
- ❖ Static structure, no moving parts, hence, no noise.
- ❖ Longer life with little maintenance because of no moving parts.
- ❖ highly mobile and portable because of light weight [21].

2.4 Demerits of Photovoltaic (PV) Panels

- ❖ The enormous demerits of Photovoltaic (PV) panels is their limited efficiency levels; compared to other renewable energy sources such as solar thermal. The efficiency of PV rages from 12 – 20 %.
- ❖ Solar Photovoltaic (PV) panels' demerits also includes it inability to store excess amounts of produced energy for later use [22].

11

2.5 Reasons for Choosing PV System

Some of the basic and common reasons for preferring a PV system are [23]:

❖ **Cost**- Solar PV system is the best cost-effective power generating system especially for addressing electricity to the remote area.

❖ **Reliability**-Since PV system has no moving parts, the chance of damage is less. As a result, the cost of maintenance is less compared to other generating systems.

❖ **Modularity-** The increased power demand of the area can be solved by adding extra modules to an existing PV system.

❖ **The environmental effect-**Solar PV system generates power without disturbing and polluting the surrounding environment.

❖ **Ability to combine systems**- It can be integrated with other types of power generating systems (wind, hydro, diesel, etc.)

Grid connected PV systems in the world account for about 99% of the installed capacity compared to stand alone systems, which use batteries. Battery-less grid connected PV are cost effective and require less maintenance. Grid-connected PV does not require batteries because the power produced is uploaded to the grid for immediate transmission, distribution, and consumption. This eases the burden on other sources supplying power to the grid [3].

2.6 Particle Swarm Optimization

Integration of PV system to the distribution system is an action to support the main grid ability of power supply. To integrate PV system first, the researcher must have known the optimal size of PV system. There are different types of algorithm which is used to get the optimal size and location of PV system. These algorithms are GA (genetic algorithm), bee colony, particle swarm optimization (PSO) and in this research work PSO technique is used to size the PV system.

2.6.1 Definition of PSO

PSO is a robust stochastic optimization technique based on the movement and intelligence of swarms. PSO applies the concept of social interaction to problem solving. It was developed in 1995 by James Kennedy (social-psychologist) and Russell Eberhart

12

(electrical engineer). It uses a number of agents (particles) that constitute a swarm moving around in the search space looking for the optimum solution. Each particle treated as a point in a N-dimensional space which adjusts its "flying" according to its own flying experience as well as the flying experience of other particles. Each particle keeps track of its coordinates in the solution space which are associated with the best solution (fitness) that has achieved so far by that particle. This value is called personal best, P_{best}. Another best value that is tracked by the PSO is the best value obtained so far by any particle in the neighborhood of that particle. This value is called G_{best}. The basic concept of PSO lies in accelerating each particle toward its P_{best} and the G_{best} locations, with a random weighted acceleration at each time step. Each particle tries to modify its position using the following information: the current positions, the current velocities, the distance between the current position and P_{best}. the distance between the current position and the G_{best} [24].

Comparing to another algorithms, Particle Swarm Optimization [25] has the flexibility to control the balance in the search space and PSO overcomes the premature convergence problem and enhances the search capability. Here the solution quality doesn't rely on the initial population.
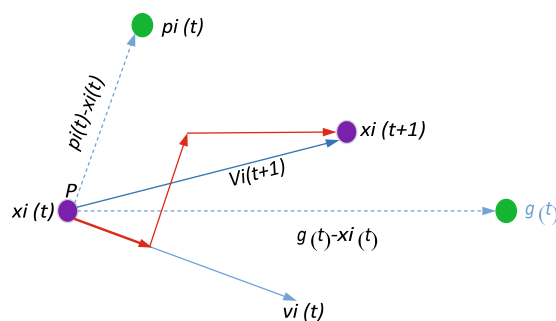
Figure 2. 1: Graphical representation of PSO

The modification of the particle's position can be mathematically modeled according the following equation:

$$V_i^{k+1} = \omega^k V_i^k + C_1 rand_1 * \left(P_{besti}^k - X_i^k \right) + C_2 rand_2 * (G_{best}^k - X_i^k) \qquad (2.1)$$

$$X_i^{k+1} = X_i^k + V_i^{k+1} \qquad (2.2)$$

13

Where, ω is the inertia weight, C_1 and C_2 are the acceleration constants. Parameters C_1 and C_2 control the rate of relative influence of the memory of other particles and their typical values are $C_1 = C_2 = 2$,

$rand_1$ and $rand_2$ are any two random numbers between 0 and 1,

V_i^{k+1} is modified velocity of particle i,

V_i^k is current velocity of particle i at iteration k,

P_{besti}^k is The personal best of particle i,

X_i^k is the current position of particle i at iteration k,

X_i^{k+1} is the modified position of particle i,

G_{best}^k is the global best of the group.

The following weight function is used:

$$W_k = W_{max} - \frac{W_{max} - W_{min}}{k_{max}} * k \tag{2.3}$$

W_{max} and W_{min} are the minimum and maximum weights respectively.

k and k_{max} are the current and maximum iteration[15].

2.6.2 PSO Algorithm

Step 1: Input line data, bus data, PV data, voltage limits, line limits and PSO settings.

Step 2: Identify the best location for Solar PV placement by the calculation of total active power loss of the system and connect the Solar PV to that particular bus.

Step 3: Calculate the base case power flow with Solar PV connected at the identified bus.

Step 4: The population of N particles is initialized with random positions, x and the velocity, v of each particle is set to zero. Each particle can have d number of variables.

Step 5: The objective function is evaluated with all particles in order to find the objective value. If the value of a particle and the objective value obtained from that particle are within the limit, that particle will be accepted. Otherwise, new particle will be generated and this step will be repeated. Then P_{best} is set as the current position and G_{best} is set as the best initial particle.

Step 6: The new velocity, vi+1 and the new position, xi+1, is calculated using equations (2.1) and (2.2) and the values of the current G_{best} and P_{best}.

Step 7: Evaluate the objective values of all particles using the new position.

Step 8: The objective value of each particle is compared with its previous objective value. If the new value is better than the previous value, then update the P_{best} and its objective value with the new position and objective value. If not, maintain the previous values.

Step 9: Determine the best particle of the whole updated population with the G_{best}. If the objective value is better than the objective value of G_{best}, then update G_{best} and its objective value with the position and objective value of the new best particle. If not, maintain the previous G_{best}.

Step 10: If the stopping criterion is met, then output G_{best} and its objective value; otherwise, repeat step six.

Step 11: Display the optimal solution to the target problem. The best position gives the location for Solar PV resulting in minimum total active power loss for the system [24].

2.6.3 Advantages and Disadvantages of PSO

PSO technique is a powerful technique for solving the non-linear optimization problems. It has its own advantages and disadvantages.

A. **Advantages of the PSO algorithm** [26]**:**
  ❖ PSO technique is a gradient-free technique.
  ❖ It is applied both in scientific research and engineering problems as the implementation of this algorithm is easy.
  ❖ Compared to other optimization techniques, this algorithm has less impact of parameters to the optimal solution as it has only less number of parameters.
  ❖ Simple calculation.
  ❖ Optimum value can be obtained easily within a short time.
  ❖ Compared to other optimization techniques, PSO has less need on a set of initial values.
  ❖ The simple concept is involved here.

B. **Disadvantages of the PSO algorithm:**
  ❖ The speed and direction may be degraded as this technique suffers from partial optimism.
  ❖ Non-coordinate system exit problem may occur.

15

2.7 Effects of connecting PV system to the grid

The grid may experience various negative effects from photovoltaic installations if the penetration of PV is very high. They are:

i. Power Quality problems/Harmonics

ii. Reverse power flow

iii. Overvoltage along Distribution feeders

iv. Voltage control difficulty

v. Phase unbalance

vi. Increased Reactive power and

vii. Islanding detection difficulty. This paper considers the Power Quality problems (Harmonics).

Power quality can be defined from two different perspectives, depending on whether supply (utility) or consume (end user) electricity. Power quality on generator(utility) refers to generator's ability to generate power at 50Hz, with little variations. While power quality transmission and distribution (end user) levels refer to the voltage staying within 5% tolerance. The growth in application of electronic equipment and distributed generation has concentrated the interest in power quality in recent years. Harmonics is one of the major power quality issues. It is caused by nonlinear loads like choppers, converters, inverters etc. These nonlinear loads produce harmonic currents and inject them into the supply system. This reduces the overall efficiency of the system [27].

2.8 Harmonics

Harmonics are measured in integer multiples of the fundamental supply frequency. Harmonics are periodic sinusoidal distortions of the supply voltage or load current caused by nonlinear loads. Harmonics occur when power supplies, variable frequency devices or other electronic devices are integrated into the system.

2.8.1 Measuring parameters of harmonics

The result of harmonics is measured by the following methods.

A. Total Harmonic Distortion (THD) is identified by Harmonic Distortion Factor which is the most common technique to calculate harmonics distortion of current and voltage.

Total harmonic distortion is the ratio of the rms value of total harmonic component of the output voltage and its rms of the fundamental component. It is a measure of closeness in a shape between the output voltage waveform and its fundamental component. [28]. THD is determined by:

$$THD = \frac{\sqrt{\sum_{n=2}^{N} V_n^2}}{V_1} \qquad (2.4)$$

Where, V_n is the rms voltage at harmonic, N is the maximum harmonic order and V_1 is the line to neutral rms voltage.

B. Total Demand Distortion: - THD can also be applied to study the current distortion stages but in the case of low fundamental load current, it can be deceiving. A small current may carry high THD which is danger for system. For example, speed drive shows the high THD values at very light loads for any value of input current. The magnitude of harmonic current is low. This high THD value for input current is not considerable concern even though its comparative distortion to the fundamental frequency is high. TDD is scientifically calculates:

$$TDD = \frac{\sqrt{\sum_{n=2}^{N} I_n^2}}{I_R} \qquad (2.5)$$

Where I_R is the peak hours demand load current at the fundamental frequency component determined at point of joint coupling (PCC). There are two ways of calculating I_R. With the load which is already in the system, it can be determined simply by averaging the peak demand current for the preceding 12 months [29].

The inverter forms the core of the grid connected PV system and is responsible for the quality of power injected into the grid. Inverters also introduce harmonics into the system in the presence of non-linear loads, during DC to AC conversion. Harmonic currents introduce voltage drop and result in distortion of supply voltage. Harmonics can also cause resonance in the supply system, resulting in malfunction, reduction in lifetime or permanent damage of electrical equipment [30].

2.8.2 IEEE standard for harmonic

Industries used harmonics standard, these standards have been developed by IEEE industry applications society and the IEEE power engineering society. This harmonic standard is

IEEE Std 519-1992. This standard has been used limits on the harmonic currents that a user can induce back into the utility power system and also specifies the quality of the voltage that the utility should supply the user. Table 3.1 below shows the harmonic current limits based on the size of the load with respect to the size of the power to which is connected [31]. The ratio I_{SC}/I_L is the ratio of the short- circuit current available at the point of common coupling to the maximum fundamental load current.

Table 2. 1: IEEE 519-1992 Voltage distortion limits (<69kV)

Bus Voltage at PCC	Individual Harmonic Distortion (%)	Total Harmonic Distortion (%)
Below 69 KV	3	5
69 KV to 161 KV	1.5	2.5
161 KV and above	1	1.5

Table 2. 2: IEEE 519-1992 Current harmonics limits (<69kV)

Maximum harmonic current distortion in percent of I_L						
Individual harmonic order (odd harmonics)[a,b]						
I_{SC}/I_L	h<11	11<h<17	17<h<23	23<h<35	35<h	THD
$< 20^C$	4.0	2.0	1.5	0.6	0.3	5.0
20<50	7.0	3.5	2.5	1.0	0.5	8.0
50<100	10.0	4.5	4.0	1.5	0.7	12.0
100<1000	12.0	5.5	5.0	2.0	1.0	15.0
<1000	15.0	7.0	6.0	2.5	1.4	20.0

*a*Even harmonics are limited to 25% of the odd harmonic limits above.

*b*Current distortions that result in a dc offset, e.g., half-wave converters, are not allowed.

*c*All power generation equipment is limited to these values of current distortion, regardless of actual I_{SC}/I_L.

Where, I_{SC} = maximum short-circuit current at PCC

I_L = maximum demand load current (fundamental frequency component) at the PCC under normal load operating conditions

2.8.3 Harmonic sources

∞ **Modern power electronic devices** such as fluorescent lamp, static power converter, arc furnace, Adjustable Speed Drives (ASDs), electronic control and Switched Mode Power Supplies (SMPS) are drawing non-sinusoidal current which contain harmonics.

∞ **Switching of power electronic devices** which includes power electric converter, controlled rectifiers, uncontrolled rectifiers, inverter, static VAR compensator, cycloconverters and High Voltage Direct Current (HVDC) transmission.

∞ **Single-phase power supplies** including personal computers, fax machines, photocopier, Uninterruptable Power Supplies (UPSs), Televisions (TVs), Video Cassette Recorders (VCRs), microwave ovens, air conditioners, electronic ballasts for high efficiency lighting and single-phase AC and DC drives [32].

2.8.4 Harmonic problems

∞ Amplification of harmonic levels resulting from series and parallel resonance.

∞ Plant mal-operation.

∞ Malfunctioning and failure of electrical equipment like transformers, cables and motors.

∞ Overheating and failure of electric motors.

∞ Overloading, overheating and failure of power factor correction capacitors.

∞ Overloading and overheating of distribution transformers and neutral conductors.

∞ Excessive measurement errors in metering equipment.

∞ Spurious operation of fuses, circuit breakers and other protective equipment.

∞ Voltage glitches in computer systems results in loss of data.

∞ Electromagnetic interference in HF communication systems such as television, radio, communication and telephone systems and similar signal conditioning devices.

∞ Harmonics increase business operating costs by increasing downtime, placing burden on the electrical infrastructure, reduce system capacity, increase maintenance, increase replacement Costs of equipment failing prematurely, making power factor correction difficult and causing poor power factor [32].

2.8.5   Influence of power inverters

Conventional inverter technology uses a centralized topology, feed by several PV panels whereas micro-inverter technology uses a distributed inverter topology, with an inverter associated with each individual PV panel. Two stage topologies is the most common topology for microinverter where maximum power from source is boosted to suitable high voltage at first stage and then converter to AC in second stage. The internal design of the power inverters including the switching topologies and the modulation techniques have a direct impact on the quality of the output waveforms and consequently their harmonic levels [33]. PV inverters influence the harmonics levels in the network by acting as source of harmonics current and by changing the effective network impedance as seen by other harmonics sources. Current THD is generally higher in single and three phase microinverter at low power output. Inverter output current THD can be reduced by implementing phase skipping control in DC link voltage controller [34]. Although several improved converter topologies such as multi-level converters or matrix converters can offer improved waveforms with lower total harmonic distortion, those topologies impose higher costs and larger size of the converter along with more sophisticated control algorithms as compared to conventional converters [35].

Additionally, several advanced modulation techniques and switching frequency are utilized to eliminate or mitigate the harmonic contents of the output waveforms of the three phase micro-inverters.

2.8.6   Harmonic Mitigation Techniques

Harmonic elimination techniques are used to improve the system power factor, to compensate the reactive power and to maintain a particular THD limit in current harmonic distribution. One of the major mitigation techniques of harmonics is usage of filters. There are generally three types of harmonic filters are used in power system:

    A. Passive filters

    B. Active filters and

    C. Hybrid filters

2.8.6.1 Passive filter

Passive filter is a combination of series/parallel connection of passive elements such as capacitors, inductors and/or resistor. They are used to inject a series high impedance to block the harmonic currents or to generate a shunt low impedance path to change the path of the harmonic currents. So, passive filters can be installed both in shunt connection or series topology. It can only mitigate a single frequency, and it injects leading reactive current (KVAr) at all times. But it is economical if you only need to deal with a dominant harmonic in the facility. It normally can reach THD target of 20% [36].

Advantages of Passive Filters

Although passive filters don't eliminate harmonics to a greater extent yet it is used due to some prominent features which are described as under

- ➢ They are simpler to configure and construct.
- ➢ Low initial & maintenance cost (compared to APF).
- ➢ Shunt passive filters of capacitive nature provide reactive power to the nonlinear load and on the other hand improve power factor by improving current displacement factor.
- ➢ Lowering of THD in line current to a permissible limit can be possible by use of passive filter [37].

Disadvantages of Passive Filters

Some major drawbacks with passive current filters are:

- ➢ Property and characteristics of filter depends on source impedance (i.e. impedance of the system and its topology) which are subjected to variations due to external condition.
- ➢ Resonating condition in the filter may create problem with loads and network leading to voltage fluctuation.
- ➢ It basically able to remove some particular harmonic components through tuning whenever the magnitude of those harmonic component is constant and pf of the system is low.

➢ Filter response is static i.e., if load variation introduces some new harmonic components then the filter have to redesigned which increases the maintenance and operation cost of the filter.

➢ Load unbalancing or neutral shifting problems can't be solved [37].

Classification of Passive Filter

A. Passive Series Filter

A passive series filter has property of purely inductive or LC tuned characteristics. The main circuitry of passive series filter is AC line inductor and DC link filter. The operating principle of series passive filter which is connected in series such that AC line inductor improves the magnitude of inductance in system which diverts the path of current drawn in the rectifier circuit. Thus, system harmonic distortion will be going to reduced compare to previous amount of harmonic content [38].
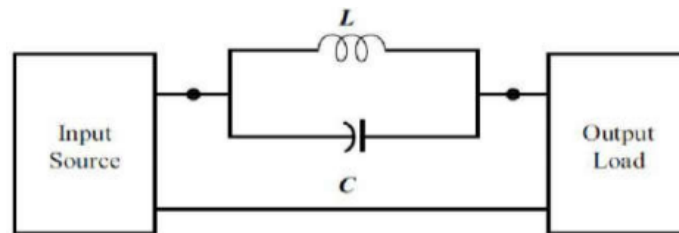
Figure 2. 2: Series Passive Filter

B. Passive Shunt Filter

Passive Shunt Filter is the most common and effective method for the mitigation of harmonic current in the distribution system. Shunt type passive filter are connected in system parallel with load. Passive filter offers a very low impedance in the network at the tuned frequency to divert the path of all the related current and at given tuned frequency. As passive filter always has tendency to offer some reactive power in the circuit so the design of passive shunt filter always carried out for the two purpose one is the filtering purpose and another one is to provide reactive power compensation for correcting power factor in the circuit at desired level. The advantage of the passive shunt type filter is that it carries just a fraction of current so that system AC power losses are reduced as compare to series type filter [38].
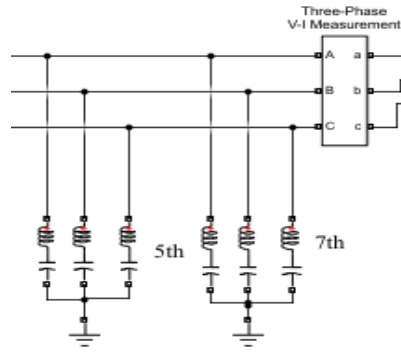
Figure 2. 3: Shunt Passive Filter

Different variety of shunt passive filters such as single tuned, double tuned, high pass and C-type filters are used for harmonic mitigation purpose but among them most commonly used filter is single tuned filter. It is very cheap and easy to design. The basic principle behind using passive filter is that at the tuned frequency filter will offer low impedance to current so that harmonic current will tends to divert in the system [38].

2.8.6.2 Active power filter

When using active harmonic reduction techniques, the improving in the power quality came from injecting equal but-opposite current or voltage distortion into the network, thereby canceling the original distortion. Active harmonic filters utilize fast-switching insulated gate bipolar transistors (IGBTs) to produce an output current of the required shape such that when injected into the AC lines, it cancels the original load-generated harmonics. The heart of the APF is the controller part. The control strategies applied to the APF play a very important role on the improvement of the performance and stability of the filter [6].

An active power filter compensates for harmonics and corrects the power factor by supplying the harmonic currents drawn by non-linear loads. Generally, the active filter is connected in parallel with the harmonic-inducing load. The APF is standard voltage source inverter having an energy storage capacitor on the dc side. The PWM (Pulse width modulation) is employed to generate gating pulse to the switches of the Active Filter. Here PI control Technique is used for providing control signal. Sensed DC voltage of the APF is compared with its set reference value in the error detector, voltage error is processed in

the PI controller according to that gating pulse are generated with pulse width modulation technique [5].

Advantages of Active Filters

➢ Widely compensated the THD in source current waveform.

➢ Only a single filter can be able to eliminate all the unwanted harmonics.

➢ Resonance condition is absent which increase the stability of power system.

➢ Filter characteristics changes with load variation due to dynamic response of the filter [37].

A. Series Active Power Filter

The Series active filter is the filter that is connected in series with the utility through a matching transformer, so it is controlled to eliminate problems related to voltage, such as voltage harmonics, voltage flicker, voltage balancing and voltage sag [39] [40].

The aim of the series APF is to locally modify the impedance of the grid. It is considered as harmonic voltage source which cancel the voltage perturbations which come from the grid or these created by the circulation of the harmonic currents into the grid impedance. However, series APFs cannot compensate the harmonic currents produced by the loads [41] [42].
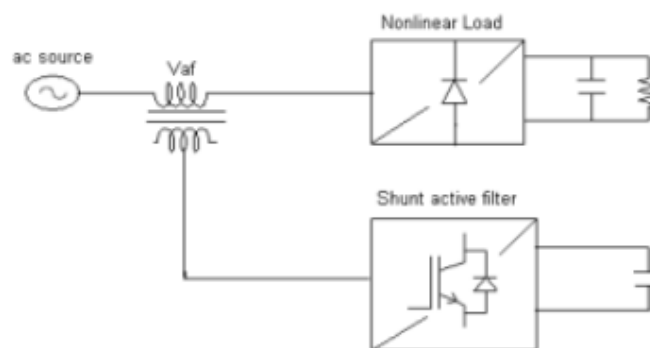
Figure 2. 4: Series Active Power Filter

B. Shunt Active Power Filter

This class of filter configurations is the most important and most widely used type in active filtering. The shunt active filter is the filter that draws a compensating current from a power line to cancel harmonic currents on the source side, a grid location where power quality

becomes important. It is widely used to eliminate current harmonics, compensate reactive power and balance unbalanced currents by injecting (drawing) additional current [40]. APF has various applications such as three-phase and single-phase, three-phase four wire system are required for voltage and current based compensation. The cost and size of the APF depends on reactive power and harmonics to be compensated [15].

The Shunt Active Power filter (SAPF) is realized by a VSI, having six numbers of IGBTs with built-in anti-parallel diodes. The SAPF is connected to the distribution AC mains through the interfacing reactor having the inductance of L_f and resistance of R_f . The real power requirement of the load is supplied from the source, the reactive power and harmonic power requirement of the load are supplied from the SAF. The capacitor C_f is connected across the DC-link of VSI [43].
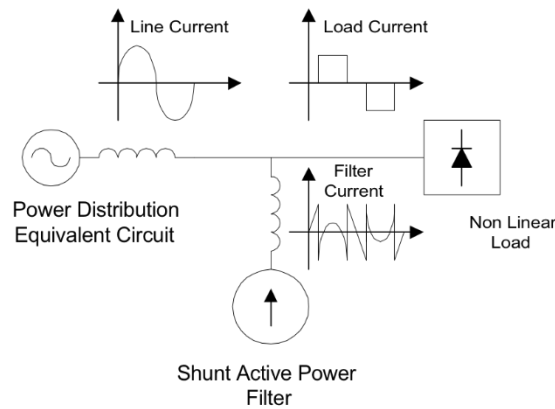
Figure 2. 5: Shunt Active Filter

2.8.6.3 Hybrid power filter

Hybrid Power Filters (HPFs) are basically consisting of Active and Passive filters which helps in considerable reduction in the rating and expenditure on filters. The voltage rating of the HAPFs is less comparatively with the active filters, Thus the cost and size of HAPFs are reduced. It also offers superior performance in flattening the harmonic voltages. PPF, a low-cost solution does not work satisfactorily under transient condition and may resonate with the grid impedance causing current amplification. While active filter is capable of compensating all the order of harmonics but their commercial use is limited due to higher cost [44]. However, the size and space acquired by passive filters is large as compared to shunt active filter. Hybrid filter topologies appears to be attractive choice,

when size, cost and reliability of the filter to be considered [45]. The main objective of the hybrid filter is to filter out predominant harmonics and avoid the resonant condition of passive filter to the grid impendence. Here, the passive filter works as Single Tuned Filter (STF) while active filter works as a Low Pass Filter (LPF).

The hybrid active filters are having more advantage in filtering harmonics than the passive filters both from feasibility and efficiency point of view, especially for high power applications [46]. Hybrid power filter retains the advantages of APF and does not have the drawbacks of PPF and APF. In Hybrid filter, the APF can improve the filter performance and suppress the harmonic resonance of existing PPF.

2.8.7   The proposed system Hybrid power filter

The system mainly consisting of Passive Filter, Active Filter, Reference current generation, PI controller, Hysteresis Current Controllers. The presented hybrid filter consists of two single tuned passive power filter tuned to the 5th and 7th component of fundamental frequency. Whereas shunt active power filter is designed to compensate higher order of harmonics. This reduces the kVA rating of shunt active filter. Active Power Filter consists of Voltage Source Converter operating at relatively high frequency to give the output which is used for cancelling low order harmonics in the power system network.
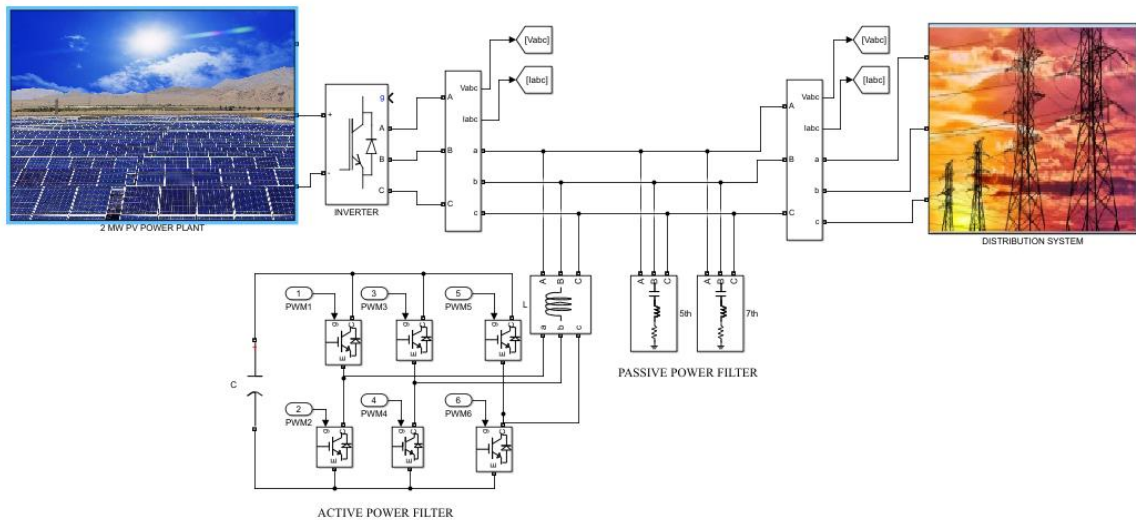
Figure 2. 6: The proposed Hybrid Power Filter

26

2.8.8 Control Techniques for Shunt Active Power Filters

The above block diagram illustrates simple Kirchhoff's current law that source current I_S will always be sinusoidal by aiding load current I_L and Compensation Current I_C. Here generating gate signals for Pulse Width Modulated VSC are main thing need to be done to operate VSC as Active Power Filter. The Block diagram for Voltage Source Converter is shown in figure 3.8. The availability of fast acting semiconductor switches like IGBTs also prefer VSC because a freewheeling diode is connected in anti-parallel with IGBT. Moreover, the recent switching stress problems are less with Voltage source Converter Compared to Current source Converter [47].
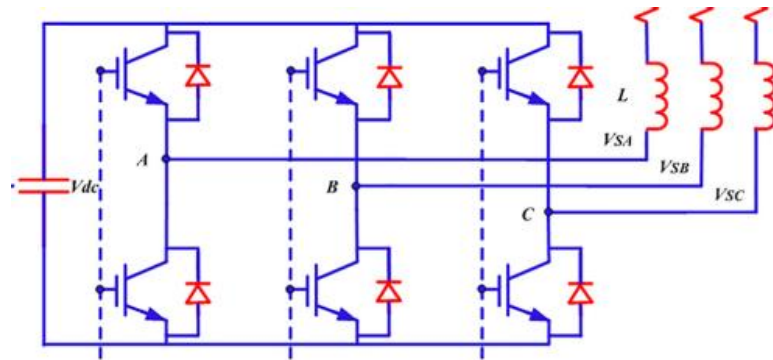
Figure 2. 7: Voltage Source Converters for SAPF

The SAF essentially contains two main sections (i) Power processing section (ii) Active filter controller section. The power processing section contains a VSI, having six IGBTs and a Capacitor (C_f) connected across the DC-link. This section performs the power processing, by synthesizing the compensating current, which has been calculated by the active filter controller section.

The active filter controller section has three main parts. (i) reference current calculation from the distorted load current (ii) the current controller for VSI (iii) voltage regulation of the DC-link capacitor [43].
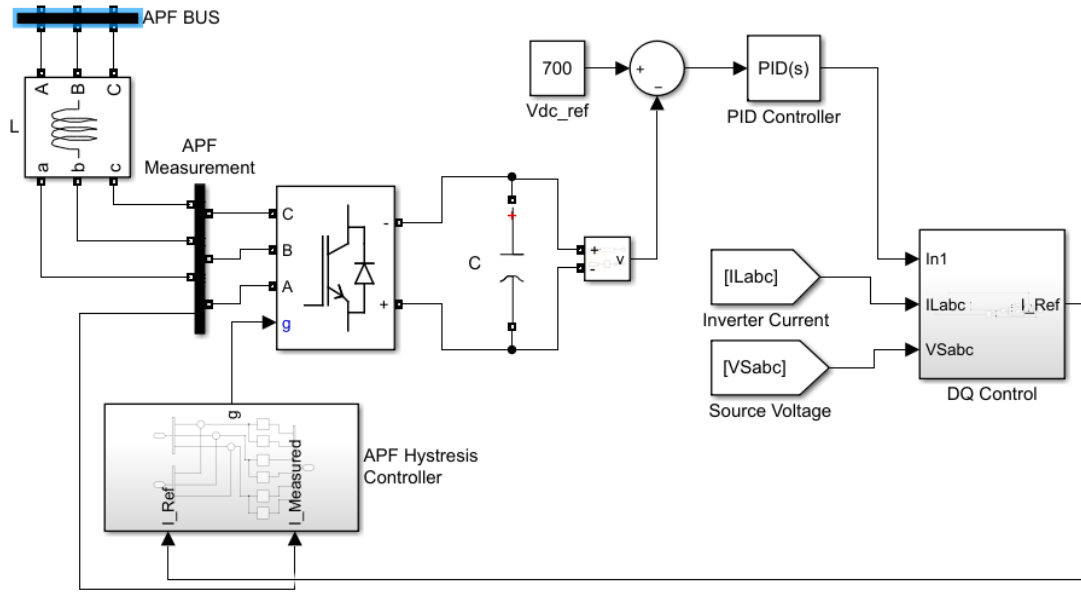
Figure 2. 8: Control of shunt active power filter

2.8.8.1 Reference Current Generation

This paper presents a method for obtaining the desired reference current for Voltage Source Converter (VSC) of the Shunt Active Power Filter (SAPF) using Synchronous Reference Frame Theory. The method relies on the performance of the Proportional-Integral (PI) controller for obtaining the best control performance of the SAPF [48] [49].

The distorted harmonic currents are first transformed into two phase stationary coordinates using ab transformation and then, these quantities are transferred into synchronous rotating frames using cosine and sine functions from the Phase-Locked Loop (PLL). Subsequently, the functions are used to maintain the synchronization with supply voltage and current. Using reference frame transformation, the reference signals are transformed from three-phase a–b–c stationery coordinate system to the 0–d–q rotating coordinate system. The harmonic component extraction using SRF theory is represented in the block diagram and is shown in Fig. 3.10.
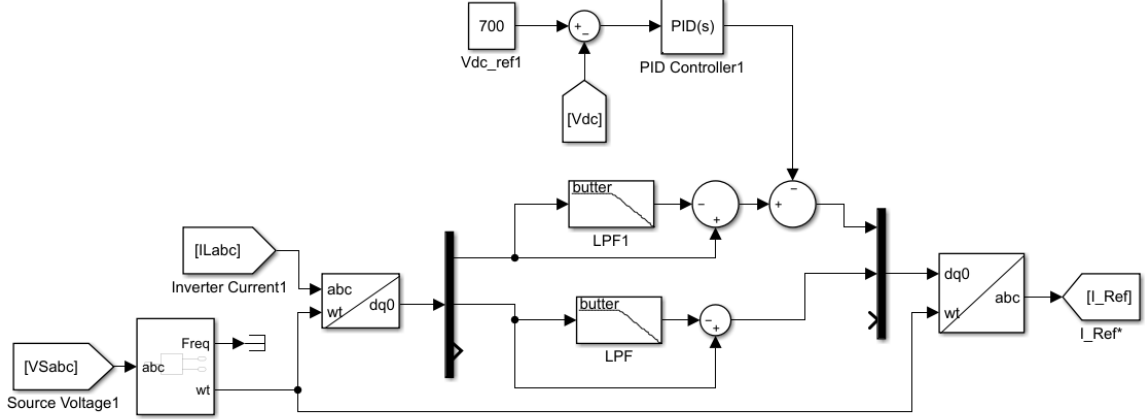
Figure 2. 9: Reference signal generation

In this scheme, the three phase load currents (i_{La}, i_{Lb}, i_{Lc}) are first sensed and transformed into two-phase frame such as direct axis (d) and quadrature axis (q) is given by (3.38)

$$
\begin{bmatrix} i_d \\ i_q \\ i_0 \end{bmatrix} = \frac{2}{3} \begin{bmatrix} \sin\theta & \sin(\theta - 2\pi/3) & \sin(\theta + 2\pi/3) \\ \cos\theta & \cos(\theta - 2\pi/3) & \sin(\theta + 2\pi/3) \\ 0 & 0 & 1 \end{bmatrix} \begin{bmatrix} i_{La} \\ i_{Lb} \\ i_{Lc} \end{bmatrix}
\tag{2.6}
$$

The d axis components are mainly used to eliminating harmonics and reactive power compensations. The output of two-phase frame depends on load current and PLL. The low pass filter is connected to filter out the higher order harmonics and allow only fundamental components. The PI controller is used to maintain the DC capacitor voltage of the three-level inverter. The error signal consists of the difference between actual voltage across the capacitor and set value. The error signal is given into PI controller. The weighted sums of these two variables are used to adjust the output process of the plant. This output is used to get the required generation of reference current for SAPF. The required reference current is calculated from i_d-i_q rotating frame using inverse transformation (3.39).

$$
\begin{bmatrix} i_{fa}^* \\ i_{fb}^* \\ i_{fc}^* \end{bmatrix} = \frac{2}{3} \begin{bmatrix} \sin\theta & \cos\theta \\ \sin(\theta - 2\pi/3) & \cos(\theta - 2\pi/3) \\ \sin(\theta + 2\pi/3) & \cos(\theta + 2\pi/3) \end{bmatrix} \begin{bmatrix} i_d \\ i_q \\ i_0 \end{bmatrix}
\tag{2.6}
$$

29

Phase-Locked Loop (PLL)

A phase-locked loop (PLL) is a control algorithm that determines the frequency and phase angle of a sinusoidal input. PLL is used for frequency matching between two systems, after which there remains a constant phase difference, hence "locking" the phase. PLL consists of a phase detection mechanism, a PID controller, and an oscillator to generate the phase angle information. In FACTS devices, PLL gain plays a vital role in stabilizing system performance [50]. The synchronizer, the Phase Locked Loop (PLL) with PI filter is used for synchronization, with much emphasis on minimizing delays.
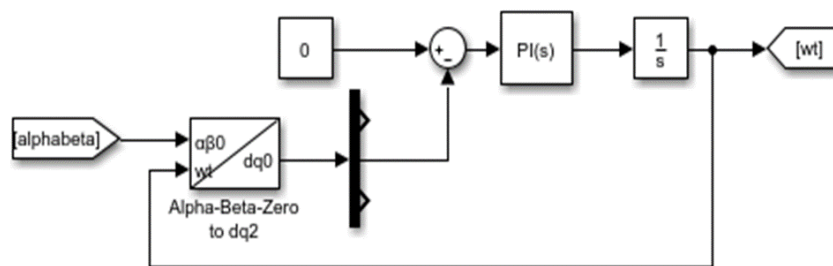
Figure 2. 10: Phase locked loop

2.8.8.2 Current controller for VSI

The steady-state and dynamic performance of the SAPF is prominently influenced by the methods applied to current control of the SAPF and the reference current calculations. Since the inverter output is continuously varying, the load current harmonics may change rapidly and the SAPF should have a faster dynamic response in current control. The hysteresis current control is implemented in this work, as it is conceptually simple, does not involve complex calculations, has a quicker dynamic response, better accuracy and can be easily implemented in the digital controllers.

Hysteresis Current Controller

Hysteresis control is simple to design and implement. Choosing the band for hysteresis control which will give satisfactory control for different operating conditions is a difficult task. PI and Hysteresis control have adopted retuning and adaptive hysteresis band approach for different operating conditions [51]**.** Compared to all current controls, Hysteresis control is simple, robust, independent of load parameter changes and has

extremely good dynamics. Also the tracking error is low and the switching pulses can be directly generated (i.e.,) no modulator is required.

The measured SAPF currents (i_{fa}, i_{fb}, i_{fc}) are compared with the reference currents (i_{fa}^*, i_{fb}^*, i_{fc}^*) in comparators. Each comparator determines the current error signal, which is given as input to the relay with a smaller hysteresis band. This relay determines the switching pulses of the IGBTs switches in the three inverter legs such that, the SAPF current is forced to remain within the desired hysteresis band. When the error signal reaches the upper bound, the switching is done to reduce the SAPF current and vice versa.

The width of the hysteresis band determines the switching frequency of the SAF [52]. The hysteresis bandwidth of 5% is chosen in this work and it results in switching frequency variation between 2 KHZ to 10 KHZ.
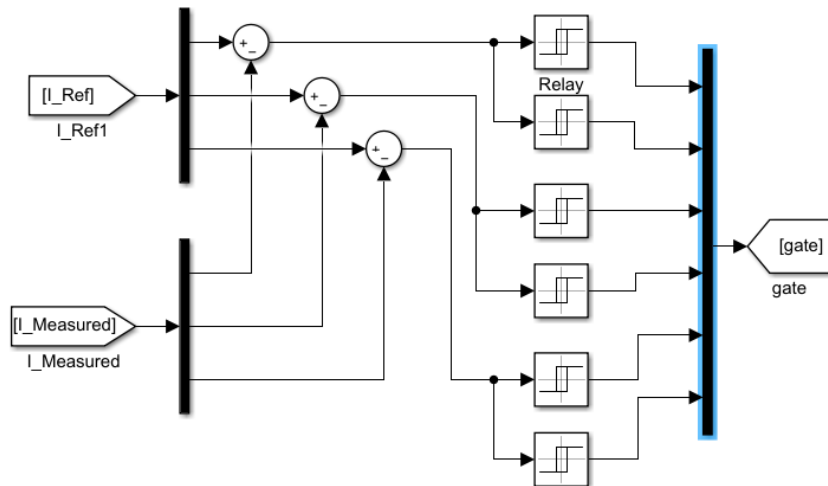
Figure 2. 11: SRFT based Hysteresis Current Controller

CHAPTER THREE

DATA ANALYSIS AND METHODOLOGY

3.1 Solar Resource Potential of the Case Study Area

It is important to assess whether solar resource is feasible or not on the specified location under study before proceed to photovoltaic power generation. Photovoltaic is a technique of producing electric power by converting the radiant energy of light in to electricity using semiconductor materials. The solar photovoltaic (PV) panel generates photovoltaic power in this process. The efficiency of a solar photovoltaic (PV) system can be affected by sunshine hour, irradiation and temperature. The solar PV module performance is generally rated under standard test conditions (STC). The standard test conditions are irradiance of 1000 W/m², solar spectrum of AM 1.5 and module temperature at 25 °C [53].

3.1.1 Sunshine Hour

Sunshine hour indicates the duration of sunshine on a specified location for a given period of time. It can be expressed as an average value for several years. The sunshine hour is taken to be 4-6 hours per day in most of the design [54]. The Ethiopian national metrology agency Bahir Dar branch has been recorded the sunshine hour of Bahir Dar city for ten years.

Table 3. 1: Monthly average sunshine hour data

	Region; Gojjam					Station: Bahir Dar						
	Element: Monthly sunshine Hour											
Month	Jan	Feb	Mar	Apr	May	Jun	Jul	Aug	Sep	Oct	Nov	Dec
2010	9.3	10.0	8.8	8.6	8.7	7.1	3.8	5.1	6.2	8.8	10	10.3
2011	9.8	10.0	8.8	8.8	7.7	7.0	4.7	4.1	5.7	8.8	9.6	9.6
2012	9.2	8.6	9.6	8.9	8.2	6.6	4.2	4.5	5.8	8.8	9.3	10.3
2013	9.0	9.8	10.2	10.7	8.0	8.0	5.1	4.2	5.8	8.5	9.7	9.4
2014	8.0	9.0	9.2	9.0	7.2	7.6	4.1	5.1	7.7	8.2	9.0	8.5
2015	8.7	8.3	8.6	8.8	8.4	7.2	4.5	3.8	6.4	9.0	9.5	9.3
2016	9.2	10.5	8.0	9.9	8.2	7.1	5.2	4.3	6.1	9.1	9.3	9.9
2017	10.1	10.1	9.2	9.4	8.2	5.6	4.5	4.0	5.9	9.5	8.6	9.9
2018	9.7	10.1	9.3	9.8	8.6	6.6	4.2	4.3	6.8	8.3	9.7	9.9
2019	9.8	9.8	9.1	7.9	7.7	6.9	4.9	4.7	6.0	8.6	9.7	9.7

From the table 3.1 above, the monthly average sunshine hour of Bahir Dar city meets the minimum sunshine hour required for designing of solar power system. It implied that the area has untouched plenty of solar resource.

Sunshine hour and solar radiance are the two fundamental factors for solar power plant efficiency. The first factor can be defined as a climatological indicator, measuring duration of sunshine in a given period for a given location on earth, typically expressed as an average value over several years. In most deign cases, the sunshine hour is considered to be 5-6 hours per day.

The second factor is solar irradiance which is the power per unit area received from the sun in the form of electromagnetic radiation in the wavelength range of the measuring instrument.

Then, the solar insolation of the city is estimated using the Angstrom-Prescott (A-P) model.

$$H_0 = \frac{24}{\pi} G_{SC} \left(1 + \cos\frac{360 n_d}{365}\right) * \left(\cos\varphi \, \cos\delta \, \sin\omega_s + \frac{\pi\omega_s}{180^o} \sin\varphi \, \sin\delta\right) \qquad (3.1)$$

$$\text{Where } \delta = 23.45^o \sin\left(360^o\, \frac{284+n_d}{365}\right)$$

$$\cos \omega_s = -\tan\varphi\, \tan\delta$$

$$H = H_0\left(a + \frac{bn}{N}\right)$$

Gsc is the solar constant (1.367 kW/m2), φ is the latitude in degree, δ is the solar declination in degree, ωs is the sunset hour angle in degree, nd is the day of the year from January 1 to December 31 taking January 1st as 1, N is the monthly average of the maximum possible hours of sunshine, n is the monthly average of daily hours of sunshine, $H0$ is the monthly average of daily extraterrestrial solar radiation, H is the monthly average of daily global solar radiation, and a and b are empirical coefficients.
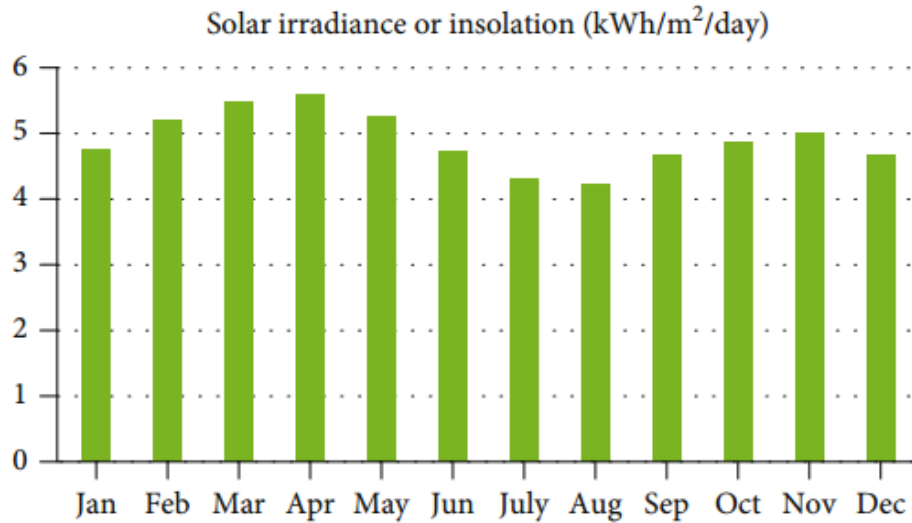
Figure 3. 1: Ten-year monthly average solar irradiance of Bahir Dar City

Using the above relation, the solar radiation of Bahir Dar City is calculated and demonstrated in Figure 3.1. The obtained solar irradiation is in the estimated range between 4 and 6 kWh/m2/day. The solar insolation data of Bahir Dar City indicates that it has much untouched potential resources for solar power plant even as compared to developed countries like Germany that uses more renewable energy resources [55].

3.2 Background of the Study Area

Bahir Dar is a capital city of Amhara region and located at latitude 11.5936403 and longitude 37.39077, in the northern hemisphere. In the city there is a rapid expansion of industrial and commercial sectors. The loads have fed from the two substations (Bahir Dar I and Bahir Dar II) which are located at Bahir Dar city. Bahir Dar sub-station II received 400 kV from Tana Beles and stepped down to 230 kV. There are two 230/132/15KV and one 230/66/15KV transformer in Bahir Dar sub-station II. These 15 kV is fed to Bata, Airforce, Industry, Abay Mado, Ghion, Tis Abay, Papyrus and Adet outgoing feeders. On the other hand, 230 kV is stepped down to 66 kV and fed to Bahir Dar sub-station I. At Bahir Dar sub-station I 66KV is stepped down to 45KV further stepped down to 15 kV. These 15 kV is fed to Semaetat, Boiler and Hamusit outgoing feeders. Nowadays these feeders are renamed as R1, R2, R3, R4, R5 and R6 for SCADA control system.
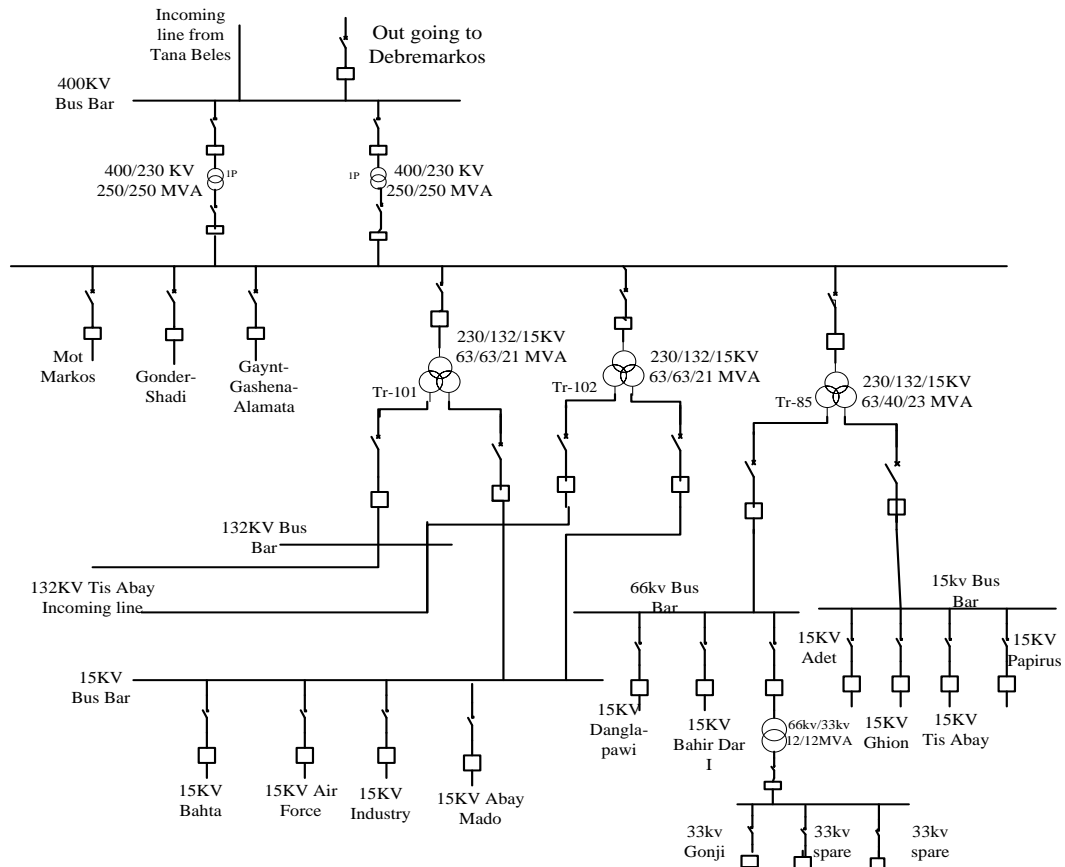
Figure 3. 2: Single Line diagram of Bahir Dar II
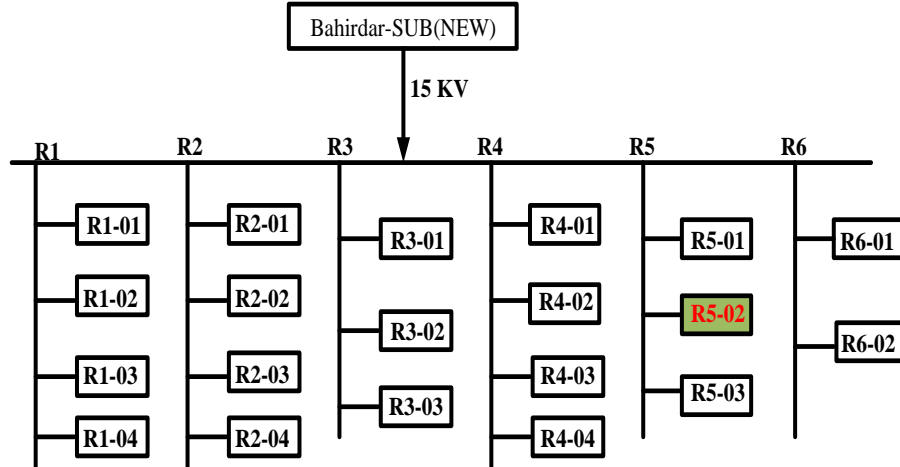
Figure 3. 3: Bahir Dar distribution system feeder

Among the twenty 15KV outgoing feeders of Bahir Dar substation, R5-02 feeder is selected for this case study due to high power interruption of the area and low voltage profile. As per data found from EEP Bahir Dar district office, the feeder has a total of 2506 customers.

The single line diagram of the network is illustrated in figure 3.4. The 28-bus system has 27 section with the total load 4.4206 MW and 2.0905 MVAr. Bus-1 is taken as a reference node or slack bus. The feeder is stranded conductor of type AAC-25, AAC-50 AAC- 95, AAC-150 and UG-Cable-300. These overhead lines are used to distribute medium voltage (15 kV) power from Bahir Dar Substation-II to the distribution transformers. The line and load data of this feeder are also shown in Appendix C.

FEEDER R5-02
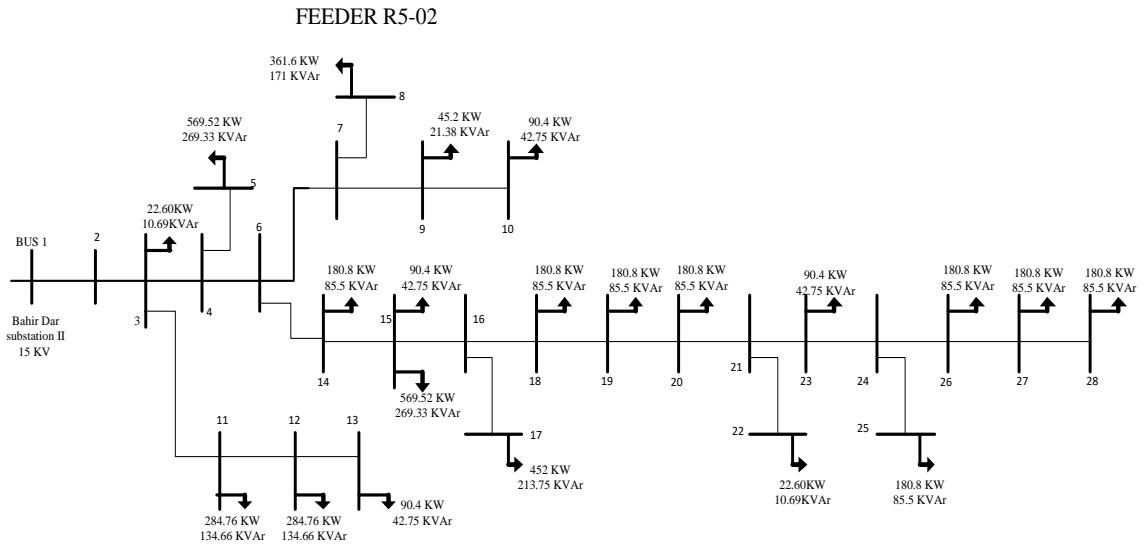
Figure 3. 4: Single line diagram of R5-02 feeder

3.3 Impedance Calculation of Overhead Distribution Line

The impedance of the overhead transmission line can be calculated using the value of manufactures resistance per using length and the length of the line. The inductance of a transmission line depends upon the material, dimensions, and configuration of the wires and length with the spacing between them. AC resistance of a conductor is always higher than its DC resistance due to the skin effect forcing more current flow near the outer surface of the conductor. Skin effect increases at high frequency. Wire manufacturers usually supply tables of resistance per unit length at common frequencies 50 or 60 Hz. The conductors that are used in distribution feeders are stranded conductors. The inductive reactance is calculated at a frequency of 50Hz, and at a length of one kilometer. Conductors used in R5-02 feeder are stranded conductors of type AAC-25, AAC-50, AAC-95, AAAC-150 and UG-Cable-300. The positive sequence impedance of the line segments is the product of the impedance per kilometer and the length of segment. The shunt admittance of overhead lines is neglected for short transmission line. The line data of the network is calculated using the table data shown in table 4.2. The resistance per kilometer of each conductor is collected from the manufacturers' data sheet.

37

Table 3. 2: Overhead medium voltage conductor size

Conductor type	Nominal area (mm$_2$)	Resistance (Ω/km)	Reactance (Ω/km)
AAC	25	1.338	0.38
AAC	50	0.68	0.362
AAC	95	0.339	0.337
AAAC	150	0.2195	0.2798
UG-Cable	240	0.1613	0.1055
UG-Cable	300	0.0789	0.1019

The values of R_L and X_L can be calculated using R_0 (ohm/km) and X_0 (ohm/km) for each type of the distribution line branch as follows:

$R_L = (R_0 \times$length of the line branch$)$ (3.2)

$X_L = (X_0 \times$length of the line branch$)$ (3.3)

The base values for both apparent power and voltage are chosen as shown below.

Sbase = 100 MVA (common power)

Vbase = 15 KV (system voltage as common)

The line and load data of the feeder R5-02 given in Appendix C is used for load flow analysis. Backward/forward load flow method is used as explained in chapter 3 to analyze the power loss and voltage profile.

3.4 Load flow analysis of radial distribution network

Load flow studies are performed on power systems to understand the nature of the installed network. Load flow is used to determine the static performance of the system. A power-flow study usually uses simplified notation such as a one-line diagram and per-unit system, and focuses on various forms of AC power (i.e.: voltages, voltage angles, real power and reactive power). It analyzes the power systems in normal steady-state operation. The distribution networks because of the some of the following special features fall in the category of ill-condition.

❖ Radial or weakly meshed networks

❖ High resistance to reactance ratios

❖ Multi-phase, unbalanced operation

- ❖ Unbalanced distributed load
- ❖ Distributed generation

Due to the above factors the Newton Raphson and other transmission system algorithms are failed with distribution network. So the backward forward sweeping method is introduced to analyze the distribution network. This method do not need Jacobian matrix unlike NR methods [56]. The backward forward sweep method is based on Kirchhoff's laws. This method has various advantages such as high efficiency of computation and requirement of memory is less. The convergence characteristic of this method is strong.

In [57], Backward-Forward Sweep load flow method uses a load-impedance matrix for fast and computationally efficient calculation of bus voltage magnitude in radial and weakly meshed distribution grids. The forward sweep calculates basically the node voltage from the sending end to the far end of the feeder and laterals, and the backward sweep is primarily calculating the branch current and/or power summation from the far end to the sending end of the feeder and laterals. In some algorithms the backward sweeps can also computed node voltages [58].

Advantage

- ❖ Jacobian Matrix is Not Needed
- ❖ Not Depends on PV and DG Number for small Networks
- ❖ Suitable for online and offline Problems

Disadvantage

- ❖ Unsuccessful for Heavy Load
- ❖ Unsuccessful for large scale network [59]

Algorithm for Forward Backward Sweep Method:

In this algorithm, the equivalent current injection (ECI), the bus-injection to the branch-current matrix (BIBC) and the branch-current to the bus-voltage matrix (BCBV) are utilized [59].

For bus-i, the complex load S_i is expressed as,

$$S_i = P_i + jQ_i \tag{3.4}$$

Where; i = 1, 2, 3... N

Equivalent Current Injection

From the specified complex power S_i at bus-i which is expressed in equation (3.4), the respective equivalent current injection based model which is practical.

From equation 2.2, the equivalent current injection is expressed as

$$I_i = I_i^r(V_i) + jI_i^i(V_i) = \left(\frac{P_i + jQ_i}{V_i}\right)^* \tag{3.5}$$

For the load flow solution, the equivalent current injection at the kth iteration at the ith node is expressed as

$$I_i^k = I_i^r(V_i^k) + jI_i^i(V_i^k) = \left(\frac{P_i + jQ_i}{V_i^k}\right)^* \tag{3.6}$$

Where,

S_i is the complex power at the ith bus

P_i is the real power at the ith bus

Q_i is the reactive power at the ith bus

V_i^k is the bus voltage at the kth iteration for ith bus

I_i^k is equivalent current injection at the kth iteration for ith bus

I_i^r is the real part of the equivalent current injection at the kth iteration for ith bus

I_i^i is the imaginary part of the equivalent current injection at the kth iteration for ith bus

3.4.1 Formation of BIBC Matrix/Backward Sweep
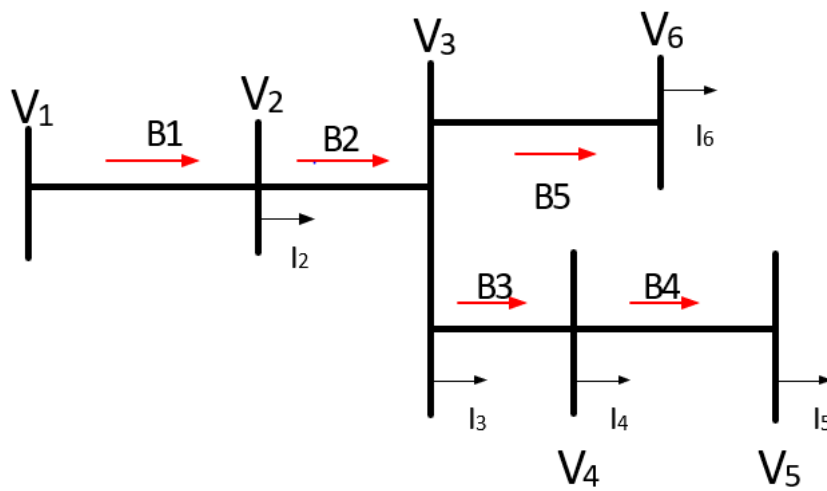
Figure 3. 5: Sample radial Distribution network

The branch currents are obtained as a function of injected currents at each bus by applying Kirchhoff's current law (KCL) to the radial distribution network as shown above in figure 3.5.

The injected currents at each bus are calculated using equation (3.5) and the branch currents B_5, B_4, B_3, B_2, and B_1 can be formulated as a function of the equivalent current injections and expressed as shown below.

$$B_5 = I_6 \tag{3.7}$$

$$B_4 = I_5 \tag{3.8}$$

$$B_3 = I_4 + I_5 \tag{3.9}$$

$$B_2 = I_3 + I_4 + I_5 + I_6 \tag{3.10}$$

$$B_1 = I_2 + I_3 + I_4 + I_5 + I_6 \tag{3.11}$$

Thus, the bus current injections and branch currents (BIBC) matrix can be expressed from the above equations (3.7-3.11) as,

$$\begin{bmatrix} B_1 \\ B_2 \\ B_3 \\ B_4 \\ B_5 \end{bmatrix} = \begin{bmatrix} 1 & 1 & 1 & 1 & 1 \\ 0 & 1 & 1 & 1 & 1 \\ 0 & 0 & 1 & 1 & 0 \\ 0 & 0 & 0 & 1 & 0 \\ 0 & 0 & 0 & 0 & 1 \end{bmatrix} \begin{bmatrix} I_2 \\ I_3 \\ I_4 \\ I_5 \\ I_6 \end{bmatrix} \tag{3.12}$$

The general form of (3.12) can be expressed as:

[B]=[BIBC][I]   (3.13)

Where; BIBC is the bus injection branch current for the given sample network is given by

41

$$[BIBC] = \begin{bmatrix} 1 & 1 & 1 & 1 & 1 \\ 0 & 1 & 1 & 1 & 1 \\ 0 & 0 & 1 & 1 & 0 \\ 0 & 0 & 0 & 1 & 0 \\ 0 & 0 & 0 & 0 & 1 \end{bmatrix} \tag{3.14}$$

3.4.2 **Formation of BCBV Matrix/Forward Sweep**

The Branch-Current to Node voltage (BCBV) matrix is the relation of branch currents and bus voltages of a radial distribution network that can be obtained by applying Kirchhoff's Voltage Law (KVL) [60].

As shown in Figure 3.5, the voltages of Node 2, 3, and 4 for the relationship between branch currents and bus voltages are expressed as:

$$V_2 = V_1 - (Z_{12}B_1) \tag{3.15}$$

$$V_3 = V_2 - (Z_{23}B_2) = V_1 - (Z_{12}B_1) - (Z_{23}B_2) \tag{3.16}$$

$$V_4 = V_3 - (Z_{34}B_3) = V_1 - (Z_{12}B_1) - (Z_{23}B_2) - (Z_{34}B_3) \tag{3.17}$$

$$V_5 = V_4 - (Z_{45}B_4) = V_1 - (Z_{12}B_1) - (Z_{23}B_2) - (Z_{34}B_3) - (Z_{45}B_4) \tag{3.18}$$

$$V_6 = V_3 - (Z_{36}B_5) = V_1 - (Z_{12}B_1) - (Z_{23}B_2) - (Z_{36}B_5) \tag{3.19}$$

Where; V_i is the voltage at bus i and Z_{ij} is the line impedance between bus i and bus j.

From equations (3.15-3.19), the node voltage of the network can be expressed as a function of the branch currents, line parameters, and main substation voltage.

$$\begin{bmatrix} V_1 \\ V_2 \\ V_3 \\ V_4 \\ V_5 \end{bmatrix} = \begin{bmatrix} V_1 \\ V_1 \\ V_1 \\ V_1 \\ V_1 \end{bmatrix} - \begin{bmatrix} Z_{12} & 0 & 0 & 0 & 0 \\ Z_{12} & Z_{23} & 0 & 0 & 0 \\ Z_{12} & Z_{23} & Z_{34} & 0 & 0 \\ Z_{12} & Z_{23} & Z_{34} & Z_{35} & 0 \\ Z_{12} & 0 & 0 & 0 & Z_{36} \end{bmatrix} \begin{bmatrix} B_1 \\ B_2 \\ B_3 \\ B_4 \\ B_5 \end{bmatrix} \tag{3.20}$$

$$[BCBV] = \begin{bmatrix} 1 & 0 & 0 & 0 & 0 \\ 1 & 1 & 0 & 0 & 0 \\ 1 & 1 & 1 & 0 & 0 \\ 1 & 1 & 1 & 1 & 0 \\ 1 & 0 & 0 & 0 & 1 \end{bmatrix} \begin{bmatrix} Z_{12} & 0 & 0 & 0 & 0 \\ 0 & Z_{23} & 0 & 0 & 0 \\ 0 & 0 & Z_{34} & 0 & 0 \\ 0 & 0 & 0 & Z_{35} & 0 \\ 0 & 0 & 0 & 0 & Z_{36} \end{bmatrix} \tag{3.21}$$

$$[BCBV] = \begin{bmatrix} 1 & 1 & 1 & 1 & 1 \\ 0 & 1 & 1 & 1 & 1 \\ 0 & 0 & 1 & 1 & 0 \\ 0 & 0 & 0 & 1 & 0 \\ 0 & 0 & 0 & 0 & 1 \end{bmatrix} \begin{bmatrix} Z_{12} & 0 & 0 & 0 & 0 \\ 0 & Z_{23} & 0 & 0 & 0 \\ 0 & 0 & Z_{34} & 0 & 0 \\ 0 & 0 & 0 & Z_{35} & 0 \\ 0 & 0 & 0 & 0 & Z_{36} \end{bmatrix} \tag{3.22}$$

$$[BCBV] = [BIBC]^T[ZD] \tag{3.23}$$

Equation (3.20) can be expressed as

$$
\begin{bmatrix} V_1 \\ V_1 \\ V_1 \\ V_1 \\ V_1 \end{bmatrix} - \begin{bmatrix} V_1 \\ V_2 \\ V_3 \\ V_4 \\ V_5 \end{bmatrix} = \begin{bmatrix} Z_{12} & 0 & 0 & 0 & 0 \\ Z_{12} & Z_{23} & 0 & 0 & 0 \\ Z_{12} & Z_{23} & Z_{34} & 0 & 0 \\ Z_{12} & Z_{23} & Z_{34} & Z_{35} & 0 \\ Z_{12} & 0 & 0 & 0 & Z_{36} \end{bmatrix} \begin{bmatrix} B_1 \\ B_2 \\ B_3 \\ B_4 \\ B_5 \end{bmatrix}
\tag{3.24}
$$

$$
\begin{bmatrix} V_1 \\ V_1 \\ V_1 \\ V_1 \\ V_1 \end{bmatrix} - \begin{bmatrix} V_1 \\ V_2 \\ V_3 \\ V_4 \\ V_5 \end{bmatrix} = \begin{bmatrix} 1 & 0 & 0 & 0 & 0 \\ 1 & 1 & 0 & 0 & 0 \\ 1 & 1 & 1 & 0 & 0 \\ 1 & 1 & 1 & 1 & 0 \\ 1 & 0 & 0 & 0 & 1 \end{bmatrix} \begin{bmatrix} Z_{12} & 0 & 0 & 0 & 0 \\ 0 & Z_{23} & 0 & 0 & 0 \\ 0 & 0 & Z_{34} & 0 & 0 \\ 0 & 0 & 0 & Z_{35} & 0 \\ 0 & 0 & 0 & 0 & Z_{36} \end{bmatrix} \begin{bmatrix} B_1 \\ B_2 \\ B_3 \\ B_4 \\ B_5 \end{bmatrix}
\tag{3.25}
$$

$$
\Delta V = [BCBV][B] \tag{3.26}
$$

$$
\Delta V = [BCBV][ZD][B] \tag{3.27}
$$

$$
\Delta V = [BIBC]^T[ZD][B] \tag{3.28}
$$

The general form for the bus voltage at $(k+1)^{th}$ iteration from equation (3.20) can be expressed as

$$
[V^{k+1}] = [V_1] - [BCBV][B] \tag{3.29}
$$

Equating equations (3.13) and (3.26), the relations between the node current injections and node voltages could be communicated as:

$$
\Delta V = [BCBV][BIBC][I] \tag{3.30}
$$

$$
\Delta V = [BIBC]^T[ZD][BIBC][I] \tag{3.31}
$$

And the distribution load flow matrix (DLF) is formed as:

$$
[DLF] = [BCBV][BIBC] = [BIBC]^T[ZD][BIBC] \tag{3.32}
$$

Substituting equation (3.31) into equation (3.32), we have

$$
[\Delta V] = [DLF][I] \tag{3.33}
$$

The iterative solution for the distribution system load flow can be obtained as:

$$
[\Delta V^{k+1}] = [DLF][I^k] \tag{3.34}
$$

$$
[V^{k+1}] = [V_1] + [\Delta V^{k+1}] \tag{3.35}
$$

3.4.3 Algorithm for Distribution Network Load Flow

The backward forward load flow algorithm described above may have the following steps for load flow solution of distribution networks as shown below:

Step 1: Read the line data and bus data of the distribution network.

Step 2: Calculate each node current injection matrix using equation (3.5).

Step 3: Calculate the BIBC matrix by using steps given in section 3.4.1 and determine the branch current.

Step 4: Form the BCBV matrix using steps given in section 3.4.2.

Step 5: Calculate the DLF matrix by using the equation (3.32).

Step 6: Set Iteration k = 0.

Step 7: Iteration k = k + 1.

Step 8: Update voltages by using equations (3.34) and (3.35).

Step 9: If max $(|V^{(k+1)}| - |V^{(k)}|)$> tolerance, go to step 5.

Step 10: Determine the branch currents and losses based on the final node voltages.

Step 11: Display the branch currents, losses, and node voltage magnitudes and angles.

Step 12: Stop

3.5 Optimal size and location of PV system using PSO

Objective function

As the main objective of this work is to determine the optimal location and sizing of the distributed generation in the distribution network to minimize the losses (active power loss), the following objective function is selected as:

$$F_l = \min P_{loss} = \sum_{k=1}^{ntl} |I_k|^2 * R_k \tag{3.36}$$

Where, F_l is the objective function to minimize power losses.

P_{loss} is the active power loss.

ntl is the number of lines in the distribution system.

Subjected to constraints:

$$V_i^{min} \leq V_i \leq V_i^{max} \tag{3.37}$$

$$I_i \leq I_i^{max} \tag{3.38}$$

$$V_{PV}^{min} \leq V_{PV} \leq V_{PV}^{max} \tag{3.39}$$

$$P_{PV}^{min} \leq P_{PV} \leq P_{PV}^{max} \tag{3.40}$$

44

Where,

P_{DG} : real power generations of DG. V_i : voltage magnitudes at bus i.

V_{DG} : voltage magnitudes at bus i. I_i: ith feeder current loading.

Problem Formulation

The problem formulation for the optimal location and sizing of the PV system in the distribution network to minimize the active power loss includes the power flow with and with-out distributed generation in the distribution system. The PV system is considered as active power sources at a particular voltage, which is at unity power factor. The well-known basic load flow equations are [61] [62]:

$$S_i = P_i + jQ_i = V_i I_i^* \tag{3.41}$$

$$S_i = V_i \sum_{k=1}^n Y_{ik}^* V_k^* = \sum_{k=1}^n |V_i| \, |V_k| |Y_{ik}| \angle (\delta_i - \delta_k + \theta_{ik}) \tag{3.42}$$

Resolving into the real and imaginary parts, then the power flow equations with-out DG are given as:

$$P_i = \sum_{k=1}^n |V_i| \, |V_k| |Y_{ik}| \angle \cos(\delta_i - \delta_k + \theta_{ik}) = P_{Gi} - P_{Di} \tag{3.43}$$

$$Q_i = \sum_{k=1}^n |V_i| \, |V_k| |Y_{ik}| \angle \sin(\delta_i - \delta_k + \theta_{ik}) = Q_{Gi} - Q_{Di} \tag{3.44}$$

The basic power balance equations:

$$P_{Gi} = P_{Di} + P_L \tag{3.45}$$

$$Q_{Gi} = Q_{Di} + Q_L \tag{3.46}$$

The power flow equations considering losses with DG for the practical distribution system and the DG is an active power source at unity power factor (PV generator) then flow are given as:

$$P_i + P_{DGi} = P_{Di} + P_L \tag{3.47}$$

$$Q_i + Q_{DGi} = Q_{Di} + Q_L \tag{3.48}$$

The DG is active power source only at unity power factor, So $Q_{DGi} = 0$.

$$P_i + P_{DGi} = P_{Di} + P_L \tag{3.49}$$

$$Q_i = Q_{Di} + Q_L \tag{3.50}$$

The final power flow equations for distribution system are:

$$\sum_{k=1}^n |V_i| \, |V_k| |Y_{ik}| \angle \cos(\delta_i - \delta_k + \theta_{ik}) + P_{DGi} = P_{Di} + P_L \tag{3.51}$$

$$\sum_{k=1}^n |V_i| \, |V_k| |Y_{ik}| \angle \sin(\delta_i - \delta_k + \theta_{ik}) = Q_{Di} + Q_L \tag{3.52}$$

$$\sum_{k=1}^n |V_i| \, |V_k| |Y_{ik}| \angle \cos(\delta_i - \delta_k + \theta_{ik}) + P_{DGi} - P_{Di} - P_L = 0 \tag{3.53}$$

$$\sum_{k=1}^n |V_i| \, |V_k| |Y_{ik}| \angle \sin(\delta_i - \delta_k + \theta_{ik}) - Q_{Di} - Q_L = 0 \tag{3.54}$$

$$P_i^{min} \leq P_i \leq P_i^{max} \tag{3.55}$$

$$Q_i^{min} \leq Q_i \leq Q_i^{max} \tag{3.56}$$

$$V_i^{min} \leq V_i \leq V_i^{max} \tag{3.57}$$

$$P_{DG}^{min} \leq P_{DG} \leq P_{DG}^{max} \tag{3.58}$$

Where

P_i and Q_i : real and reactive power flow at bus i. P_{Di} and Q_{Di} : real and reactive loads at bus i. V_i and V_k : voltage magnitudes at bus i and k. P_{DGi} : real power of DG at bus i.

n: total number of buses. δ_i and δ_k: voltage angles of bus i and k.

Y_{ik} : magnitude of the ikth element in bus admittance matrix.

θ_{ik} : angle of the ikth element in bus admittance matrix.

3.6 Sizing of grid interconnected solar plant

Proper sizing of the PV system is very important in order to improve the system performance. In this section, the procedure for sizing the whole grid connected solar power plant is discussed. Firstly, the inverter system is chosen as the main sizing item of the whole system. There are three types of inverter systems for grid interconnected PV plant; centralized inverter system, string inverter system and multi-string inverter system. Among these inverter systems, multi-string inverter system is the most flexible design with high efficiency. Combination of the advantages of central and string technologies makes a compact and cost-effective solution. And individual PV strings can be turned on and off to use more or fewer modules [63]. For these above advantages, multi-string inverter system is the most useful inverter system for large scale grid connected PV system. Fig.4.2 shows the multi-string inverter system for grid interconnected PV plant. To calculate the inverter input DC voltage, inverter amplitude modulation index is assumed. To process maximum power by an inverter, inverter amplitude modulation index should be at maximum value without producing unwanted harmonic distortion. Therefore, inverter amplitude modulation index should be in the range 0.95 to produce the highest AC output voltage of inverter [64].
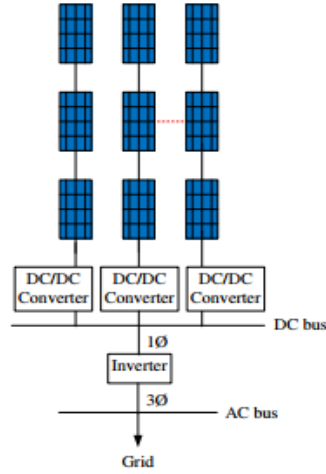
Figure 3. 6: Multi-String Inverter Topology

To size the whole grid interconnected solar photovoltaic power plant, the inverter system is firstly chosen. In this proposed system, multi-string inverter system is used. Inverter input DC voltage can be calculated by using the following equation.

$$V_{idc} = \frac{2\sqrt{2}V}{\sqrt{3}M_a}$$ (3.59)

Where, V_{idc}= Inverter input DC voltage, V = System voltage, M_a= Inverter amplitude modulation index.

Numbers of module N_m is

$$N_m = \frac{V_s}{V_{mpp}}$$ (3.60)

Where, V_s= String voltage, V_{mpp} = Voltage at maximum power point, V

String power P_s can be calculated by

$$P_s = N_m \times P_{MPP}$$ (3.61)

Where, P_{MPP} = Power at maximum power point, W

$$N_S = \frac{P_s}{P_a}$$ (3.62)

$$N_a = \frac{PV_{generation}}{P_a}$$ (3.63)

47

Where, P_a = Array power, W

Total numbers of modules can be calculated as follows:

$$Total\ numbers\ of\ modules\ =\ N_m \times N_s \times N_a \tag{3.64}$$

Boost converter output voltage is equal to the inverter input DC voltage and Boost converter input is equal to the string voltage.

$$V_o\ =\ V_{idc} \tag{3.65}$$

$$V_i\ =\ V_s \tag{3.66}$$

Where, V_o = Boost converter output voltage, V_i = Boost converter input voltage

Number of inverters is obtained by dividing the PV generation to one inverter power P_i.

$$N_i\ =\ \frac{PV_{generation}}{P_i} \tag{3.67}$$

3.6.1   Design of Boost Converter
The value of inductance and capacitance of boost converter is given by [65]:

$$Inductance,\ L = \frac{V_{ip}(V_{op}-V_{ip})}{f_{sw}*\Delta I*V_{op}} \tag{3.68}$$

$$Capacitance,\ C = \frac{I_{op}(V_{op}-V_{ip})}{f_{sw}*\Delta V*V_{op}} \tag{3.69}$$

Where, V_{ip} is the solar operating voltage, f_{sw} is the switching frequency of boost converter, V_{op} is the output voltage of boost converter or the input voltage of inverter, I_{op} is the Output current, ΔI is current ripple, ΔV is voltage ripple.
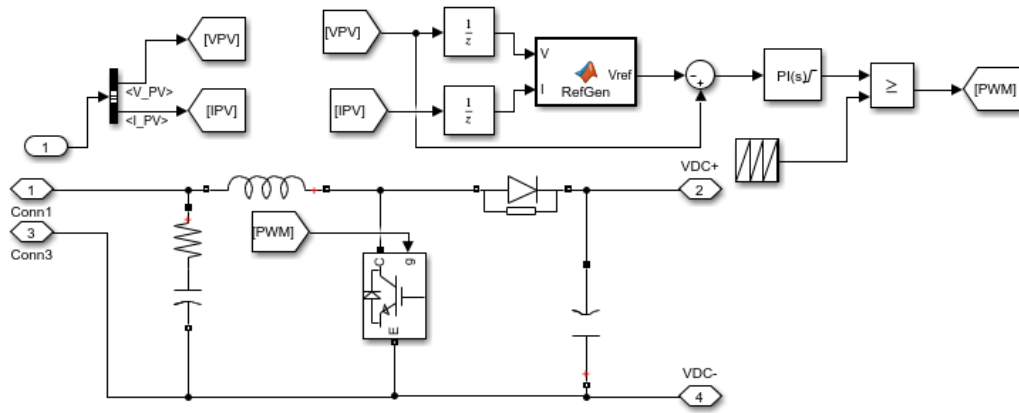
Figure 3. 7: Boost converter with MPPT

Table 3. 3: Main Parameters of the System

PV system	
Module	Tata power
Power at maximum power point	300W
Number of string(series)	16
Number of array(parallel)	58
Total number of modules	7424
DC-DC Boost Converter	
Number of converters	8
L	1.525 mH
C	3258µF
Inverter	
Number of converters	8

3.6.2 Design of Shunt Passive Filter

The following are the basic steps involved in design of single tuned or detuned power system harmonic filter calculation. These passive power filters are used in control of harmonics in industrial and commercial power systems [66].

Analyze the individual and total harmonic distortion of the inverter without filter using FFT analysis. Then the current and voltage harmonics values of each harmonics order

compared with IEEE Standard 519-1992. If the individual and total harmonic distortion is higher than IEEE standard 519-1992 the next step is designing the filter.

The passive filter used here is the single tuned passive filter. It is the simplest and easy to construct among all shunt passive filters. In this filter the inductor and capacitor are designed to mitigate a particular order of frequency by providing a low impedance path. For most harmonic filters in power systems, filters are tuned to 4.2 or 4.7 for trapping 5th order harmonics. For capturing 7th order, harmonics filters can be tuned to 6.7. These filters are often called 'detuned' filters since they are not tuned to the exact harmonic order. If a single-tuned passive harmonic filter were off tuned, its performance would be deteriorated substantially and resulted in a parallel resonance between grid inductance and filter capacitance. In order to avoid this side effect from off-tuning, the filter must be tuned on some preceded order not on the exact order. In other words, total filter impedance must have reactive impedance on a tuned frequency. The quality factor(Q), which determines the sharpness of tuning, is related with a scale which shows the degree of harmonic current absorption quantity. In this respect, all filters will be one of the high or a low Q type according to use. In passive filter design, the tuning factor and quality factor must be taken into account before calculating filter parameters (R, L and C). In this thesis, the tuning orders of 5th and 7th filters have been determined as 4.813th and 6.734th, respectively. And the quality factor (Q) has been chosen as 50 [67].

Determine the Filter Design
Step 1: Determine the effective capacity of reactive power filter (KVAR / MVAR, 3-Phase Value)**.** Usually, the effective capacity of reactive power rating is determined based on reactive power requirement of load or May be determined by harmonic duty requirements.
Step 2: Determine the frequency tuning filters
In accordance with IEEE 1531-1993, harmonic single tuned filter frequency is determined in amount of 3%- 15% below the determined frequency as safety factor. In this paper, the tuning orders of 5th and 7th filters have been determined as 4.813th and 6.734th, respectively. And the quality factor (Q) has been chosen as 50.
Step 3: Determine impedance of effective filter

$$X_{eff} = \frac{KV^2}{Q_{eff}} \tag{3.70}$$

Step 4: Determine capacitive and inductive reactance of fundamental frequency

$$X_{C1} = \frac{h_n^2}{h_n^2 - 1} X_{eff} \tag{3.71}$$

$$X_{L1} = \frac{X_{C1}}{h_n^2} \tag{3.72}$$

Where: h_n= harmonic order tuned by filter with safety factor

Value of harmonic filter reactor can be calculated using

$$X_L = 2\pi f L \tag{3.73}$$

Where f is the system frequency and L is the value of inductance needed.

Step 5: Find the characteristic reactance X_n and the resistance of reactor.

$$X_n = \sqrt{X_C X_L} \tag{3.74}$$

If Q is the filter's desired quality factor (typically between 30-100), then the resistance can be calculated as:

$$R = \frac{X_n}{Q} \tag{3.75}$$

Step 6: Determine rating of reactive power capacity of capacitor

$$Q_{Crated} = \frac{KV^2}{X_C} \tag{3.76}$$

Step 8: Voltage appearing across capacitor is

$$V_C = \frac{h_n^2}{h_n^2 - 1} V_{bus} \tag{3.77}$$

The results obtained from equation and compared with the standard IEEEE 519-1992. If the result is less than the standard, then the calculation can proceed to the next step. If the result is greater than the standard, then the calculation back to step 1.

Step 7: Determine current of nominal capacitor Current of nominal capacitor

$$I_{Nom} = \frac{Q_{Crated}}{\sqrt{3} V_{LL}} \tag{3.78}$$

3.6.3 Design of Shunt Active Power Filter

The design of 3 - phase Shunt Active Filter involves the selection of the filter inductor (L_f), dc link capacitor (C_{DC}) and power rating of the SAPF. [68]. The design presented over here is for 3-phase 3-wire system, where a VSC based inverter is used.

A. Power rating of filter (SAPF)

Filter is designed to mitigate harmonics by considering Total Harmonic Distortion along with the load power. To reduce the fundamental reactive power, sine of the fundamental phase angle is required to design the rating of the power device. The rating of the SAPF is a function of the load characteristics [69]. The power rating is given by,

$$S_{APF} = \sqrt{\frac{sin^2_{q_1}+THD^2}{1+THD^2}}\,S_{load} \tag{3.79}$$

where THD is considered for maximum load current distortion. For harmonic compensation, the rating of the filter is given by,

$$S_{APF} = \sqrt{\frac{THD^2}{1+THD^2}}\,S_{load} \tag{3.80}$$

B. Reference DC bus voltage of SAPF

Choosing the proper value of Vdc, ref, reduces the ripples of dc bus voltage [70]. The DC voltage of the bus (V_{DC}) is given by (4.49) as,

$$V_{DC} = 2\sqrt{\frac{2}{3}}V_{ll} \tag{3.81}$$

C. Design of DC link capacitor (C_{DC})

DC bus capacitance can be calculated in two different ways.

i. Using the law of conservation of energy: On application of increment or decrement of load, the capacitance DC voltage also changes. Using the energy principle and law of conservation of energy, (4.50) is written.

$$C_{DC} = \frac{3aV_{ph}It}{0.5(V^2_{DC}-V^2_{DC1})} \tag{3.82}$$

where, V_{DC} is the reference voltage and V_{DC1} is the minimum or maximum voltage level of the DC bus, a is the overloading factor, V_{ph} is the phase voltage, I is the current of VSC phase and t is the time by which the has to be recovered to the reference value.

ii. harmonic ripple voltage:

The value of dc-link capacitor can also be written as (3.83).

$$C_{DC} = \frac{I_d}{2\omega V_{DCripple}}$$ (3.83)

Where, I_d is the current of active filter, and can be expressed as (3.84).

I_d = *active filter kVA/DC link voltage* (3.84)

D. **Design of filter inductor (Lf)**

The selection of AC inductor depends on the current ripple I_{crp}, considering I_{crp} as 10% of I_d, (3.85) is written to express the value of L_f .

$$L_f = \frac{\sqrt{3}V_{DC}}{12f_s I_{crp}}$$ (3.85)

Next important aspect of select the appropriate current and voltage ratings of power electronic switches. The voltage rating $V_{sw}=V_{DC}+V_d$, where V_d is the spike in capacitance voltage during transient conditions. The current ratings of switches are calculated as, $I_{sw}=Ip+Icrp$, where, *Ip* is the peak current of SAPF [71].

Design specification

In this design the system is a grid connected solar PV system which consists of a PV panel, boost converter, inverter and grid. This system is selected to reduce the cost of the whole system by avoiding battery backup. When the battery back-up capacity is excluded, the cost of the whole system decreases by around 40 to 50% depending on the type of batteries used and the capacity required.

The network consists of a PV array, which generates peak of 2 MW. A DC/DC converter, which is also used as a power optimizer, is equipped with control functions such as Maximum Power Point Tracking (MPPT). The PV system is integrated to the grid by means of a DC/AC inverter, a step-up transformer and an evacuating line of 15 kV. The point of common coupling is Bus 20. The size of PV array 2MW and the optimal location bus 20 is found by PSO algoritm. The power is fed from PV system and the utility to the distribution network consisting of twenty-one transformers.

The system designed based on the above equations is calculated and the simulation parameters are listed in Table 3.4, Table 3.5, Table 3.6 and Table 3.7.

Table 3. 4: Design parameters of Boost converter and Inverter

Parameters	Values
Grid voltage	400V
Boost converter parameter	L= 1.525mH, C=3258µF
Load	Inverter
Inverter DC voltage (VDC)	900V
Inductance of inverter	45 µH

Table 3. 5: Shunt Passive filter parameters used for simulation

Parameter	Unit	Value
Capacity of Reactive Power Capacitor	KVAR	2090.5
Inductive Reactance (4.813)	Ω	4.8559
Inductance (4.813)	mH	15.4645
Capacitive Reactance (4.813)	Ω	112.486
Capacitance (4.813)	µF	28.312
Inductive Reactance (6.734)	Ω	2.427
Inductance (6.734)	mH	7.729
Capacitive Reactance (6.734)	Ω	110.06
Capacitance (6.734)	µF	28.94

Table 3. 6: Shunt active filter parameters used for simulation

Parameters	Values
Capacitor	8151.6 µF,
Interfacing reactor	1 mH
DC-link voltage	700 V
Rating of SAPF	71.7 KVA

Table 3. 7: Hybrid Power filter parameters used for simulation

Parameter	Unit	Value
Shunt passive filter		
Capacity of Reactive Power Capacitor	KVAR	2090.5
Inductive Reactance (4.813)	Ω	4.8559
Inductance (4.813)	mH	15.4645
Capacitive Reactance (4.813)	Ω	112.486
Capacitance (4.813)	μF	28.312
Inductive Reactance (6.734)	Ω	2.427
Inductance (6.734)	mH	7.729
Capacitive Reactance (6.734)	Ω	110.06
Capacitance (6.734)	μF	28.94
Shunt active filter		
Capacitor	μF,	2497.18
Interfacing reactor	mH	1.3
DC-link voltage	V	700
Rating of SAPF	kVA	21.96

CHAPTER FOUR
SIMULATION RESULTS AND DISCUSSION

In this research, backward forward sweep load flow analysis is implemented on the selected 28-buses radial distribution feeder of Bahir Dar city using the collected line and load data and the base case power losses and voltage profile are obtained using MATLAB R2018a software. The impact of integrating solar PV system to the distribution system in terms of power loss, voltage profile and harmonic distortion are analyzed for different penetration level of the PV system. Base MVA=100 and base KV=15 is used as system input data to convert in to per unit values. The selected radial distribution feeder has 28 bus and 27 section with the total load 4.4206 MW and 2.0905 MVAr. A PV size is considered in a range of 10 kW to 2 MW. In this study, it is considered that the PV is operated at unity power factor. The first bus is considered as the feeder of electric power from the generation/transmission network. The remaining buses of the distribution system except the reference buses are considered for the placement of a PV of given size from the range considered. Loads were modeled as constant power loads (PQ load) and were solved by using Backward Forward Sweep Load flow analysis.

4.1 Base-case Power Losses and Voltage Profile

A load flow analysis using backward/forward algorithm has been performed without connecting PV system and calculate voltage profiles at each bus and both real and reactive power losses in each line. The base case voltage profiles of the network are presented in table 4.1.

Table 4. 1: Base case voltage profile

BUS No	Voltage profile without PV	BUS No	Voltage profile without PV	BUS No	Voltage profile without PV
1	1	11	0.9498	21	0.9410
2	0.9523	12	0.9496	22	0.9410
3	0.9506	13	0.9496	23	0.9399
4	0.9486	14	0.9468	24	0.9397
5	0.9481	15	0.9465	25	0.9396
6	0.9477	16	0.9456	26	0.9382
7	0.9474	17	0.9454	27	0.9380
8	0.9469	18	0.9442	28	0.9378
9	0.9474	19	0.9429		
10	0.9473	20	0.9415		

As it can be observed the voltage profile of all buses except the first three buses are below the minimum threshold value (0.95 p.u). Bus 28 presents the lowest voltage profile which is 0.9378 p.u.

The Base Case total real and reactive power losses of the system are 182.75 KW and 264.81 KVar respectively. Optimizing to minimize the loss and maximize the voltage profile to be in the desired range needs proper sizing and placing of PV system.

4.2 Optimal Size and Location of PV System using PSO

The applied PV DG is supply active power only, while the maximum penetration level allowed is assumed to be 45.24% of the total generation [36]. The capacity of the PV DG is assumed to be in the range of 10 KW–2 MW. Buses that are located between bus 2 and 28 are considered a possible location for the PV DG unit. A constraint for bus voltage magnitude is assumed to be between 0.95 pu and 1.05 pu. The results consist of two steps. The first step is to access the best location of Solar PV and the second is the calculation of minimum active power loss.

Table 4.2 shows the suitable PV DG size of a 28 bus system and the minimum power loss occurs in bus 20 (76.8 KW and 109.93 KVar). The proposed method can reduce loss by 57.97 % real power and 58.49 % reactive power of its original loss.

Table 4. 2: Results of a 28-bus test system

| Bus No	DG Size MW	Ploss KW	Qloss Kvar	Bus No	DG Size MW	Ploss KW	Qloss Kvar
2	2	92.20	125.46	16	2	79.05	111.24
3	2	88.65	120.88	17	2	79.92	111.74
4	2	84.71	115.79	18	2	77.68	110.44
5	2	86.16	116.63	19	2	76.91	109.99
6	2	82.91	113.47	***20***	***2***	***76.80***	***109.93***
7	2	83.66	114.45	21	2	77.13	110.12
8	2	86.96	115.55	22	2	79.04	111.23
9	2	83.88	114.73	23	2	77.94	110.59
10	2	84.95	116.10	24	2	78.31	110.80
11	2	89.90	122.16	25	2	79.33	111.40
12	2	90.80	123.08	26	2	82.45	113.20
13	2	91.36	123.66	27	2	83.30	113.70
14	2	80.96	112.34	28	2	86.53	115.58
15	2	80.48	112.07				
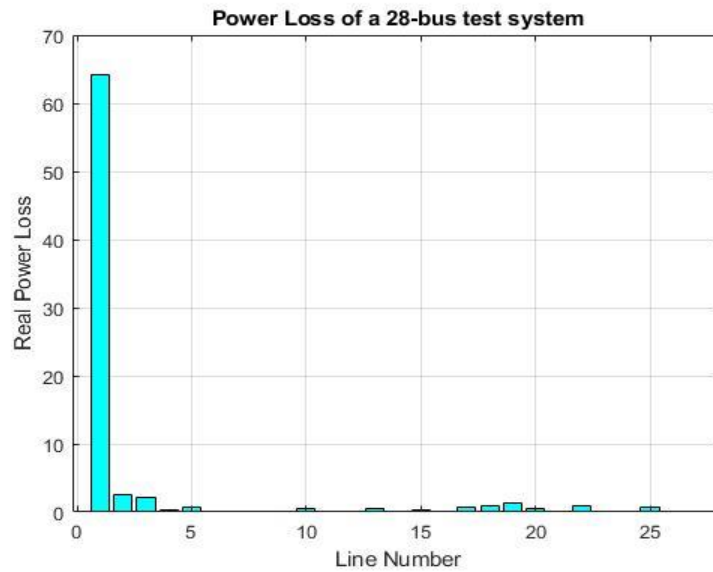
Figure 4. 1: Power loss of a 28-bus test system

Fig 4.2 shows the voltage level comparison for the 28-bus system with and without installation of PV system. The outcomes represent that installation of PV system considerably improves the voltage profile. In the system without DG units, the lowest

voltage level is 0.9378 per unit. After the PV units are installed, the voltage level are improved (0.9601 per unit).
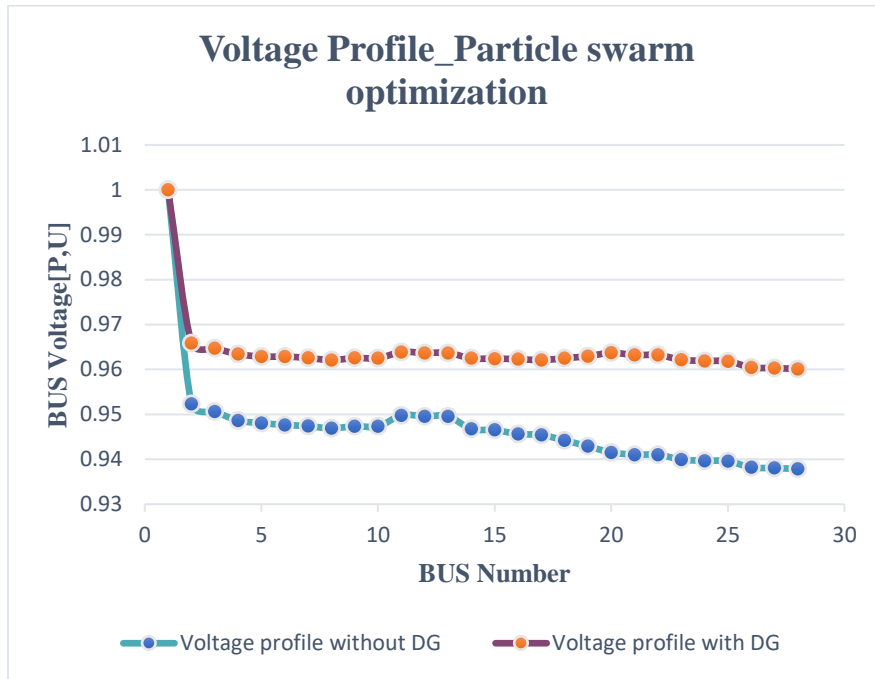

Figure 4. 2: Voltage level comparison on the 28-bus system

A Particle Swarm Optimization for optimal placement of PV system is efficiently minimizing the total real power loss satisfying transmission line limits and constraints. The methodology is fast and accurate in determining the sizes and locations. By installing PV system at all potential locations, the total power loss of the system has been reduced drastically and the voltage profile of the system is also improved.

4.3 Grid connected PV system

The grid connected PV system is simulated in MATLAB SIMULINK environment to check the total harmonic distortion of source current. The simulation is carried under two different conditions. A) without filter B) with filter

Considering the inverter as non-linear load, three cases of harmonic mitigation are compared: a) pure passive filter, b) pure shunt active power filter, b) hybrid power filter

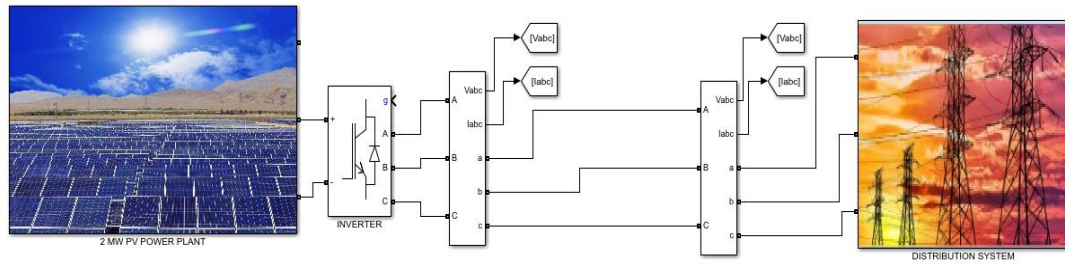### 4.3.1 Grid Connected PV system without filter

Figure 4. 3: MATLAB/SIMULINK model of grid connected PV system without filter
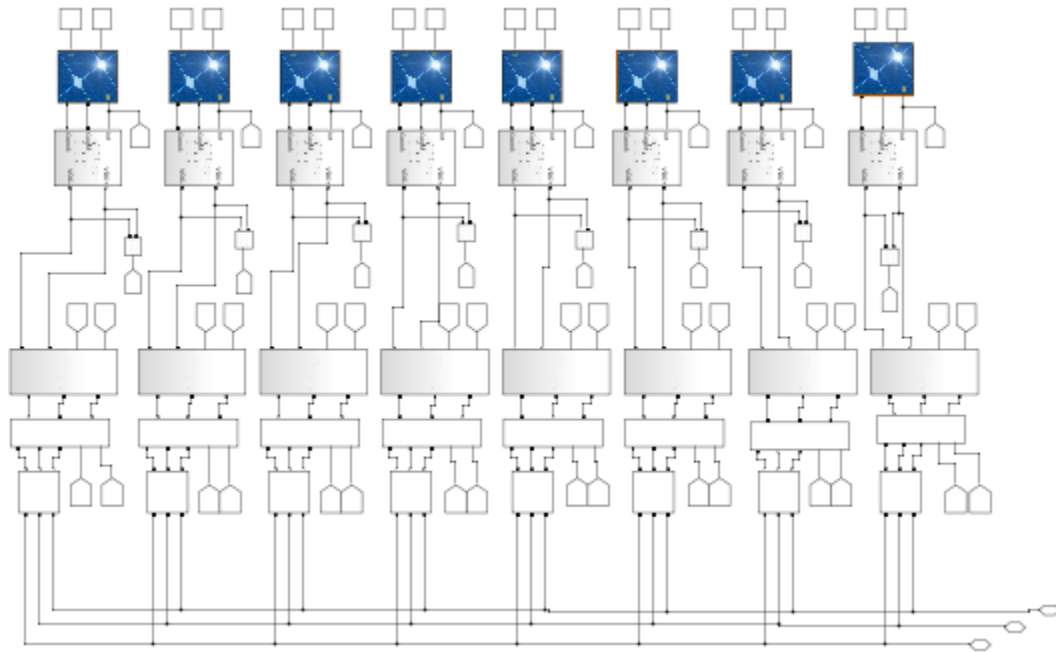
Figure 4. 4: Sub system of 2MW PV system
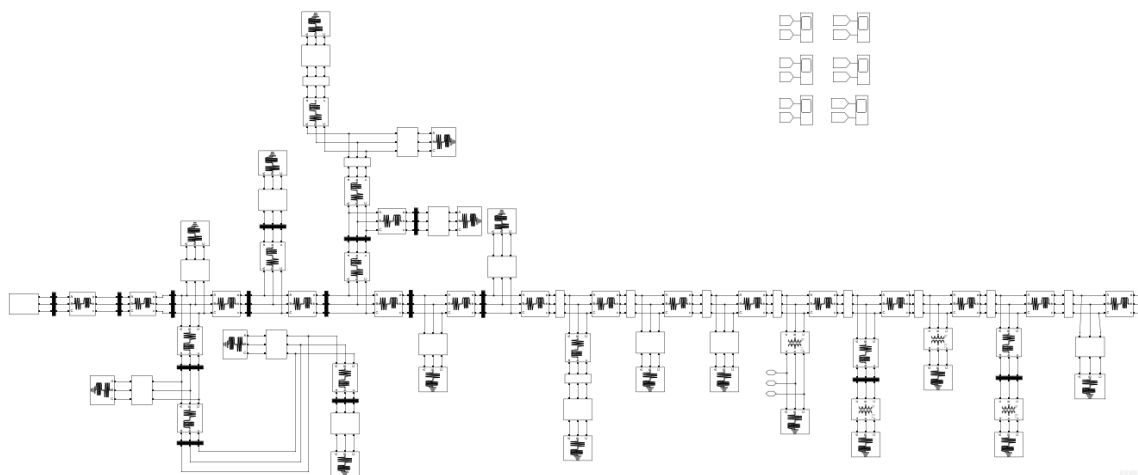
Figure 4. 5: Sub system of 15 KV distribution system
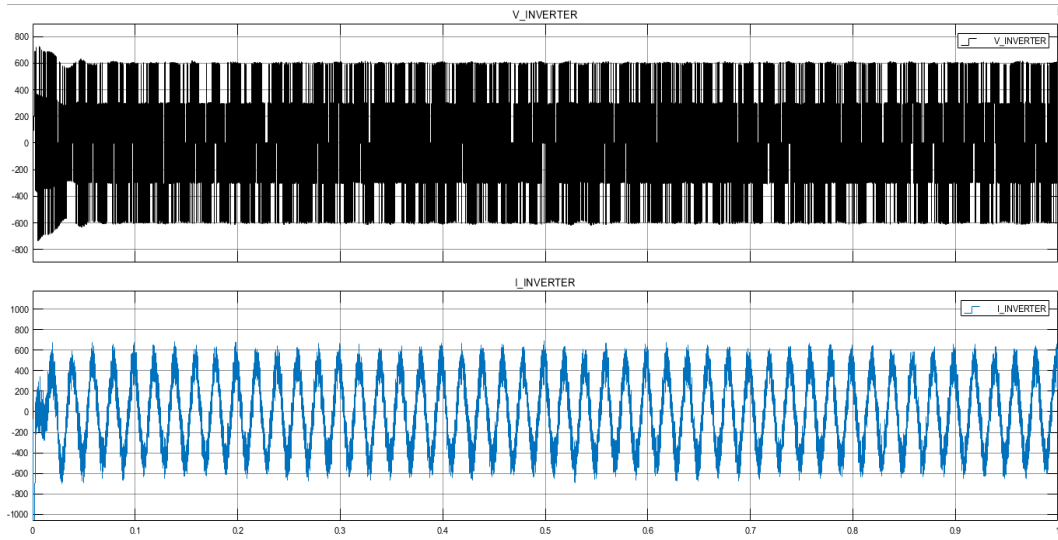
Figure 4. 6: Single phase inverter Voltage and inverter Current without filter

Figure 4.7 shows the waveform of grid voltage and current when filter is not connected in the system for filtering the harmonic current components which can be produced due to inverter. Since there is no compensation provided the inverter current waveform is exactly as grid current waveform. It can be seen that the grid current contains harmonic content and thus is not purely sinusoidal. It is cleared that the power factor will be reduced and power loss will increase in the system. It also affects the stability of grid side of the system.

a)

b)
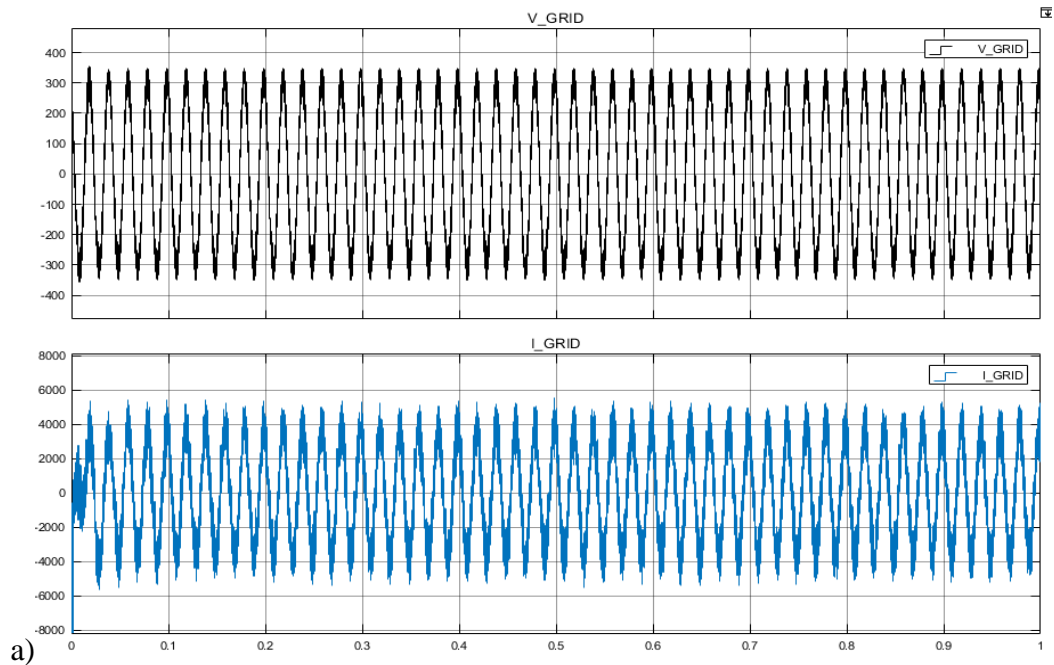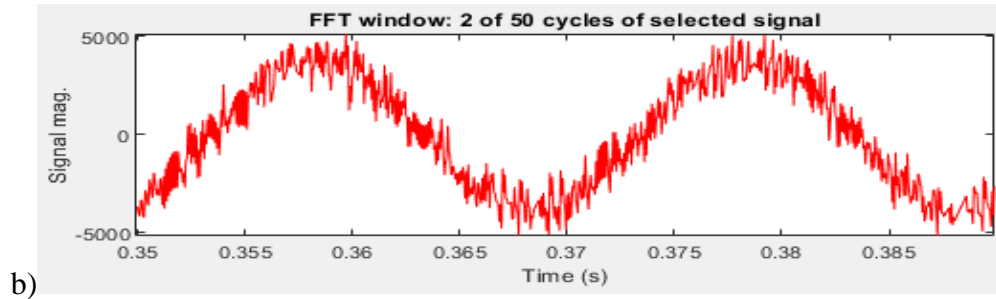
Figure 4. 7: a) Grid Voltage and Current without filter, b) 2 of 50 cycle of grid current without filter

The source current contains 29.94% THD when compensation is not provided which is above IEEE 519- 1992 standard. The FFT analysis is given in figure 4.8.
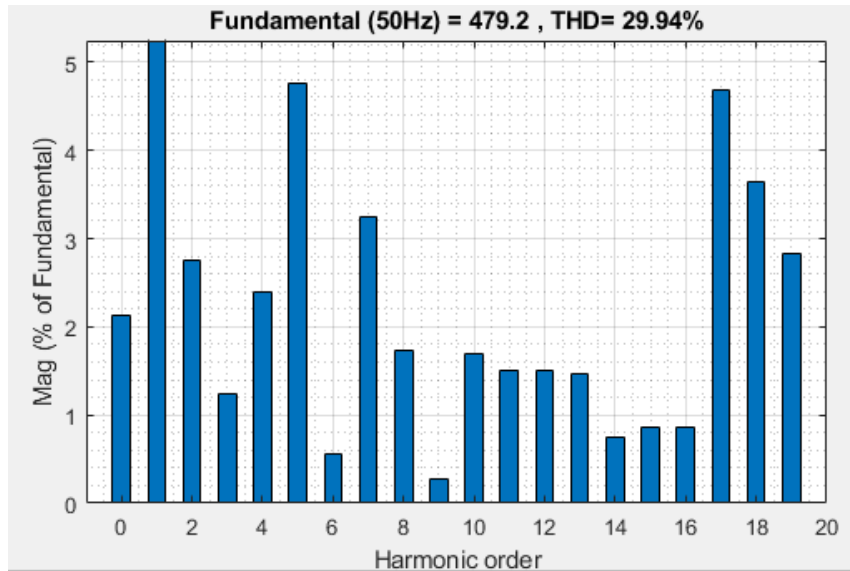
Figure 4. 8: FFT analysis of grid current without filter

Due to the inverter, grid current is distorted (figure 5.7) and inject THD of 29.94% in grid as indicted in figure 4.8.

Table 4. 3: The individual and THD of Grid current without filter

Harmonic current order	THD	3rd order	5th order	7th order	11th order	13th order	17th order	19th order
Without filter	29.94	1.24	4.77	3.25	1.51	1.47	4.68	2.83

Table 4.3 show that the 5th and 7th order have high distortion value, so shunt passive filter is designed for 5th and 7th order to reduce distortion of the two orders.
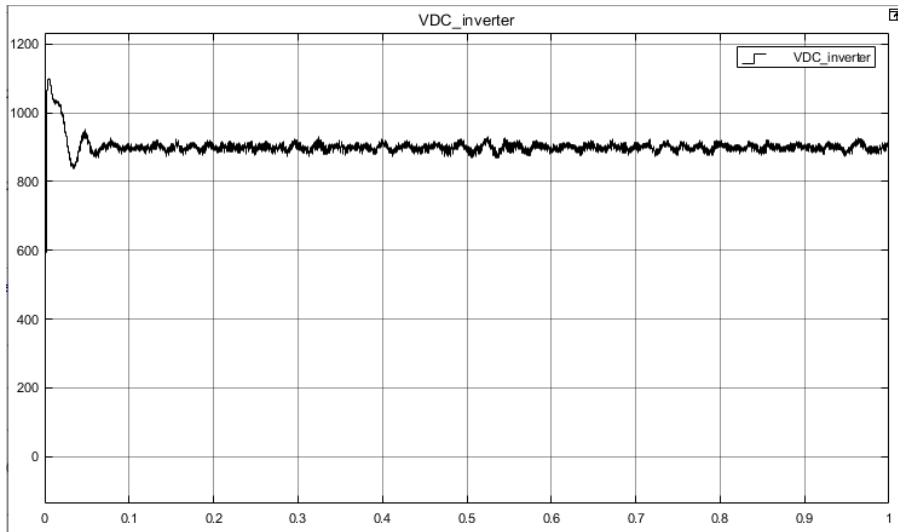
Figure 4. 9: Simulation result of Inverter DC voltage

4.3.2 Grid connected PV system with Shunt Passive filter
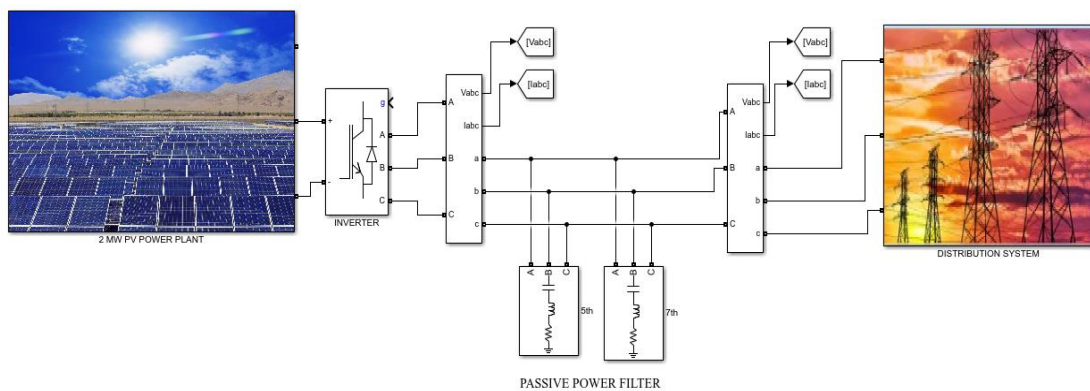
Figure 4. 10: MATLAB/SIMULINK model of grid connected PV system with shunt passive filter

When passive filter is connected to PCC, passive filter draws the harmonic current of order 5th and 7th of fundamental. This improves the nature of the grid current as shown in figure 4.12 and reduces the overall THD from 29.94 % to 8.82 % as shown in figure 4.13.
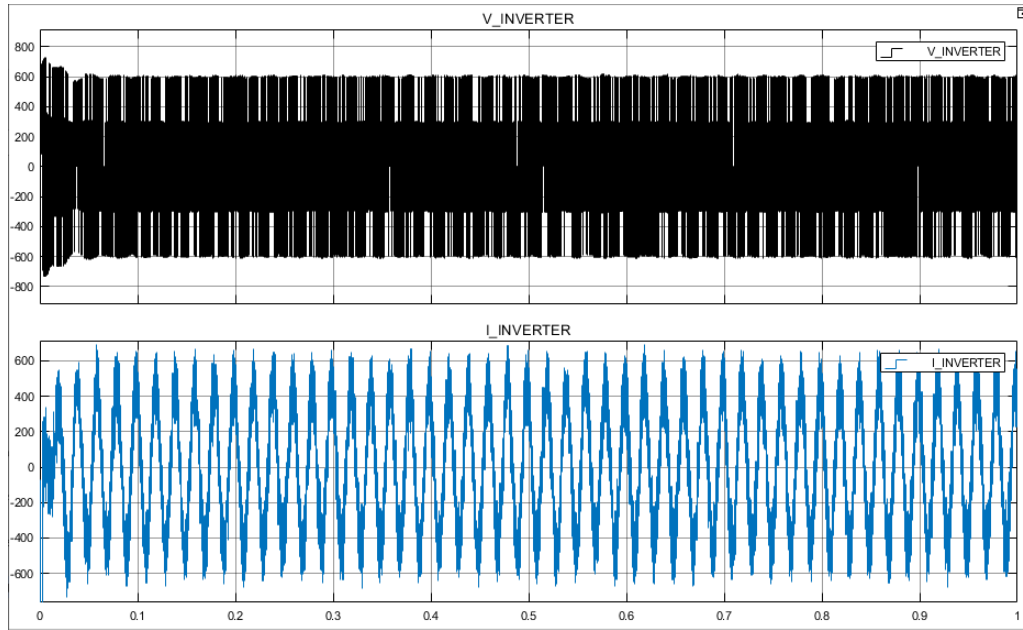
Figure 4. 11: Inverter Current and Voltage after PPF compensation

As shown in the figure 4.6 and 4.11 the Inverter current and voltage wave form before and after compensation is the same. Only the grid current and voltage wave form is changed after PPF compensation which is more close to sinusoidal wave form but not exactly the same.

a)

b)
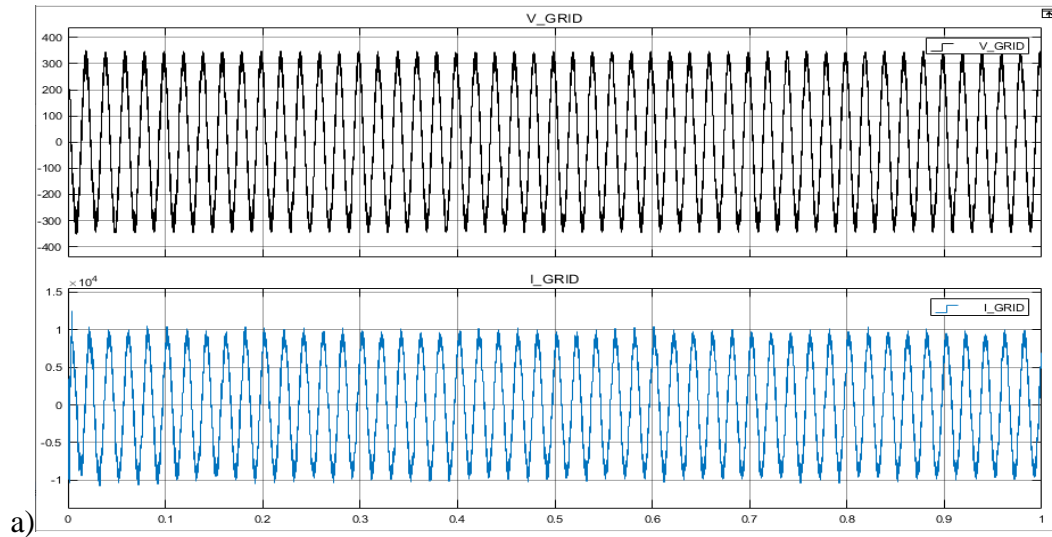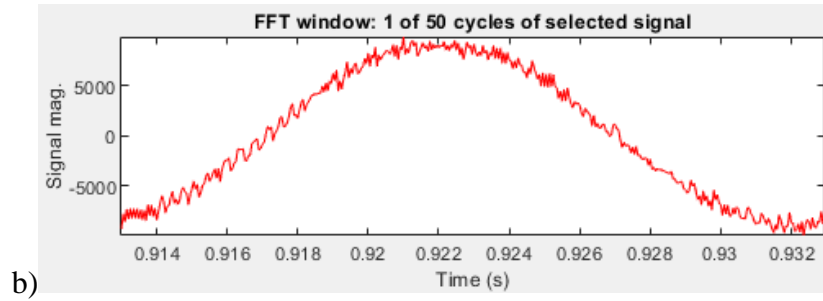
Figure 4. 12: a) Grid Current and Voltage after PPF compensation b) 1 of 50 cycle of grid current with PPF

Figure 4. 13: FFT analysis of Grid Current after PPF compensation

Table 4. 4: The individual and THD of Grid current without filter and with shunt passive filter

Harmonic current order	THD	3rd order	5th order	7th order	11th order	13th order	17th order	19th order
Without filter	29.94	1.24	4.77	3.25	1.51	1.47	4.68	2.83
With Shunt Passive filter	8.82	0.61	0.51	0.64	0.53	0.74	0.66	0.23

Table 4.4 show that the 5th order harmonics is reduced from 4.77% to 0.51% and 7th order harmonics is reduced from 3.25 to 0.64 but the THD is 8.82% which is above IEEE Standard. So, Active power filter is needed to meet the IEEE standard,

65

4.3.3 Grid connected PV system with Shunt Active Power filter
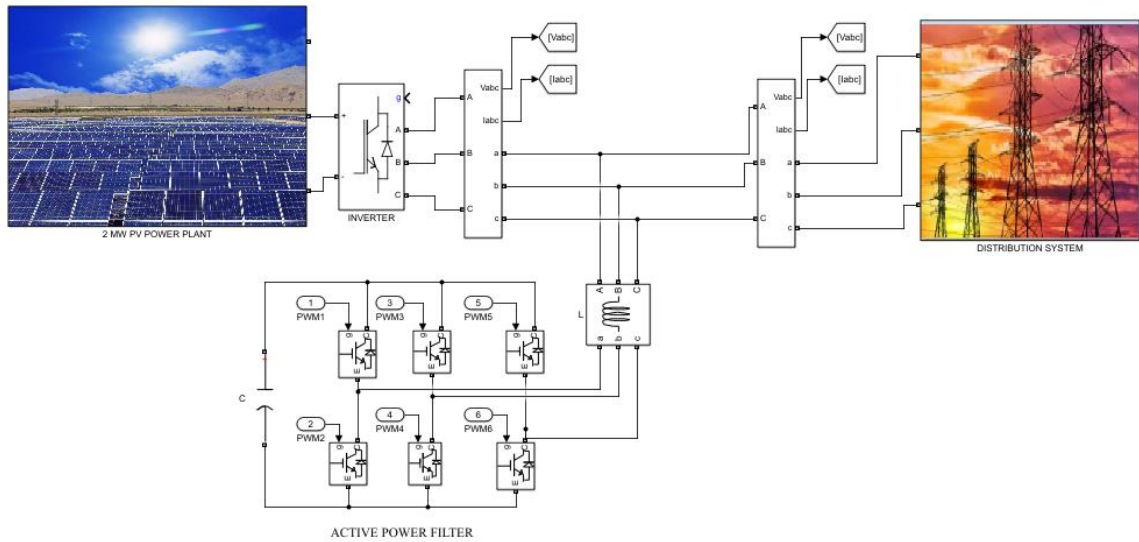
Figure 4. 14: MATLAB/SIMULINK model of grid connected PV system with shunt active filter
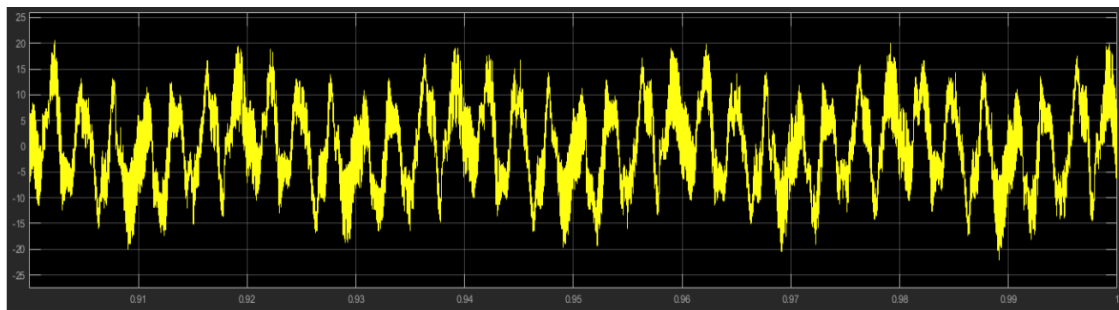
Figure 4. 15: Waveform of Shunt active filter compensation current

Figure 4.15 shows the waveform of generated filter current to compensate harmonic current which can be produced by the inverter. This filter current is injected at the Point of Common Coupling (PCC) to mitigate Total Harmonic Distortion (THD) of the system. This filter current is equal and opposite in magnitude with respect to the harmonic current which is generated by the inverter.
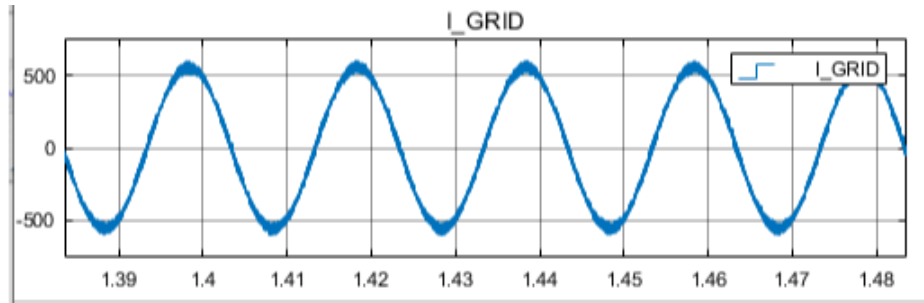
a)
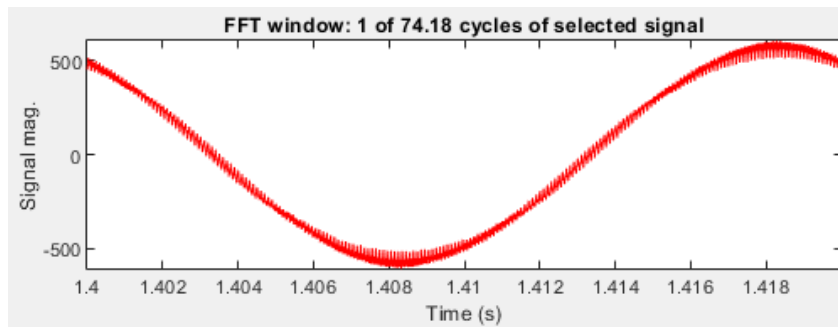
b)

Figure 4. 16: a) Simulation result of grid current when Shunt active filter is connected, b) 1 cycle of grid current after shunt active filter is connected
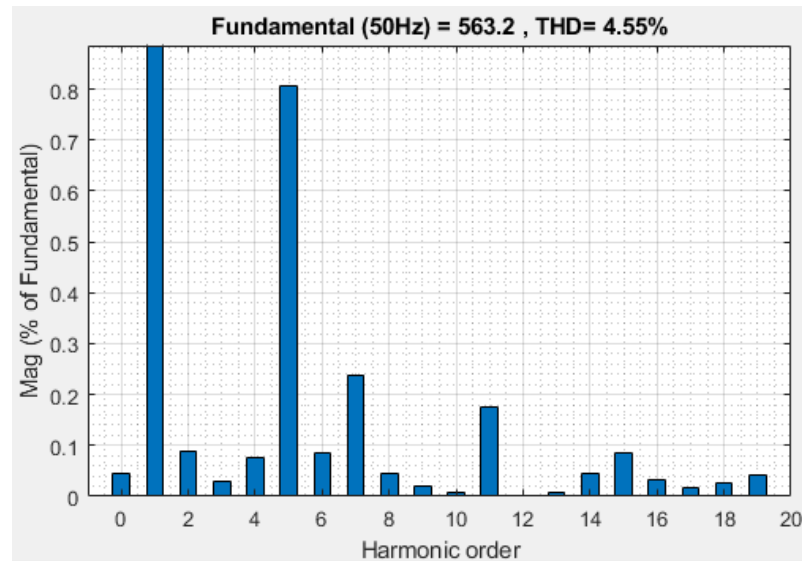
Figure 4. 17: FFT analysis of Grid Current after Shunt active filter compensation

It is clear that the when shunt active filter connected in the system, then it injects compensated current which is equal and opposite of harmonics components due to inverter in the system. The waveform has improved when hybrid filter is switched ON and the waveform of source current has become closer to sinusoidal than before compensation. The capacitor charging voltage (Vdc) which generates required current with harmonics for the compensation of reactive power is shown in figure 4.18.
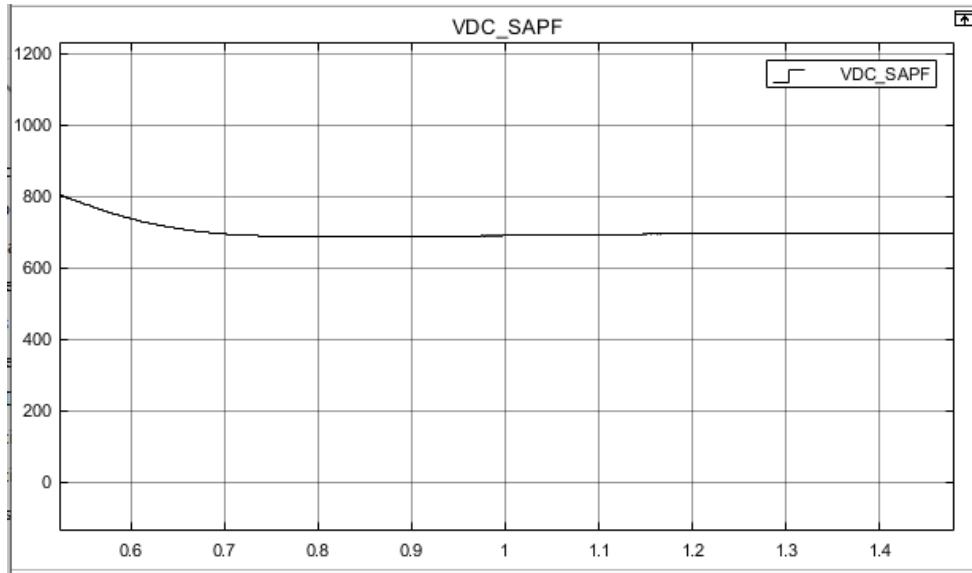
Figure 4. 18: Simulation result DC capacitor voltage of Shunt active filter
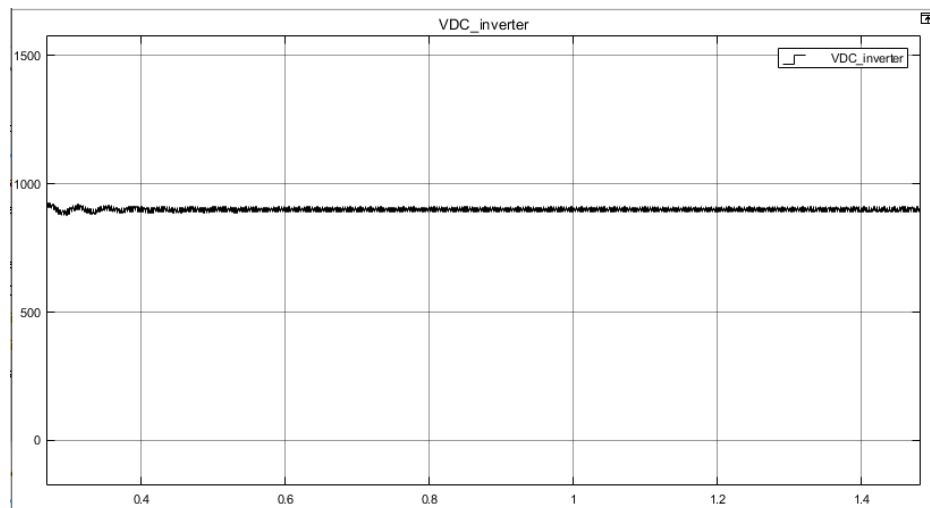
Figure 4. 19: Simulation result DC voltage of Inverter

Table 4. 5: The individual and THD of Grid current without filter and with shunt active filter

Harmonic current order	THD	3rd order	5th order	7th order	11th order	13th order	17th order	19th order
Without filter	29.94	1.24	4.77	3.25	1.51	1.47	4.68	2.83
With Shunt Active filter	4.55	0.03	0.81	0.24	0.18	0.01	0.02	0.04

Table 4.5 show that when only shunt active filter is connected at PCC, the THD of the source current is 4.55% which is below the IEEE standard. But the shunt active filter used in this case has high rating which is 71.7KVA.

4.3.4   Grid connected PV system with Hybrid Power filter

The basic circuit configuration of the line with compensation is as shown in figure 5.20. The active filter is connected in shunt with shunt connected passive filter. The MATLAB/SIMULINK is carried out with the control strategy of instantaneous reactive power theory. The gating pulses for VSI is provided by the comparison of source current and reference current with the rectangular pulse generator. Hybrid filters are usually considered a cost-effective option for power quality improvement, compensation of the poor power quality effects due to nonlinear loads, or to provide a sinusoidal AC supply to sensitive loads.
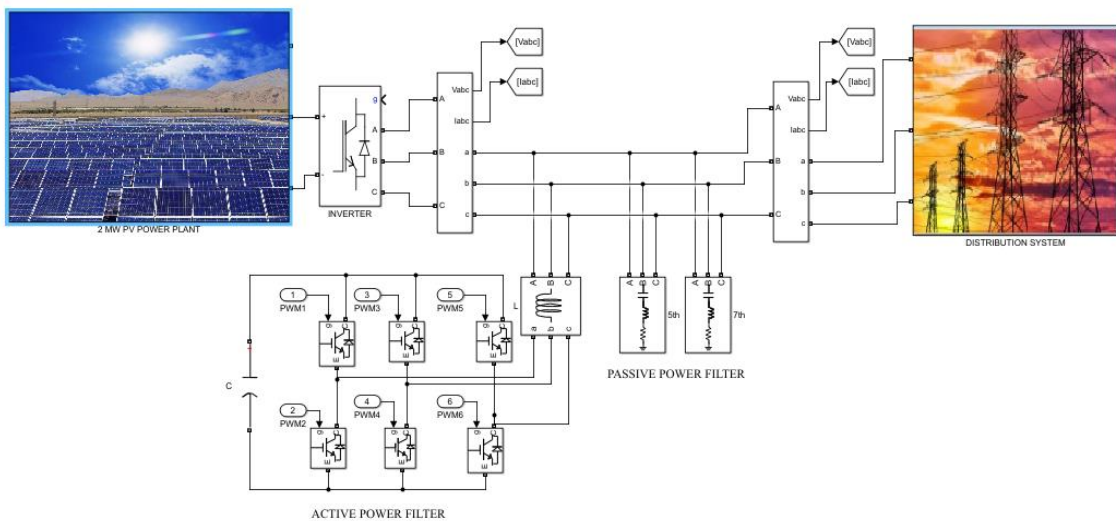
Figure 4. 20: MATLAB/SIMULINK model of grid connected PV system with Hybrid
power filter (HPF)
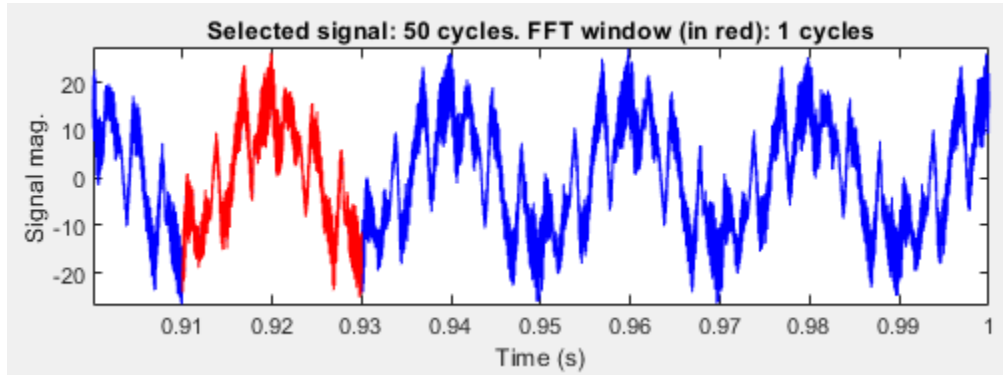
Figure 4. 21: Waveform of generated filter current when Shunt active filter is connected
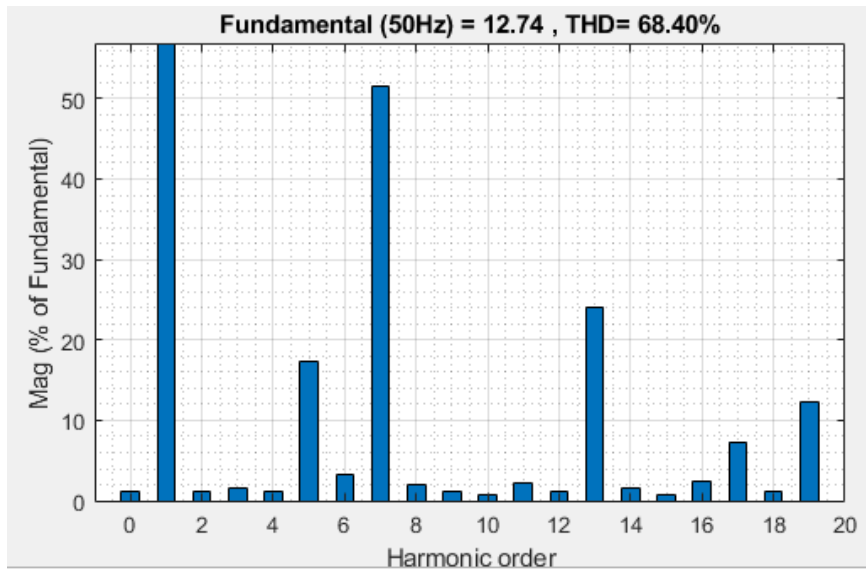
Figure 4. 22: FFT analysis of Shunt active filter compensation current in HPF
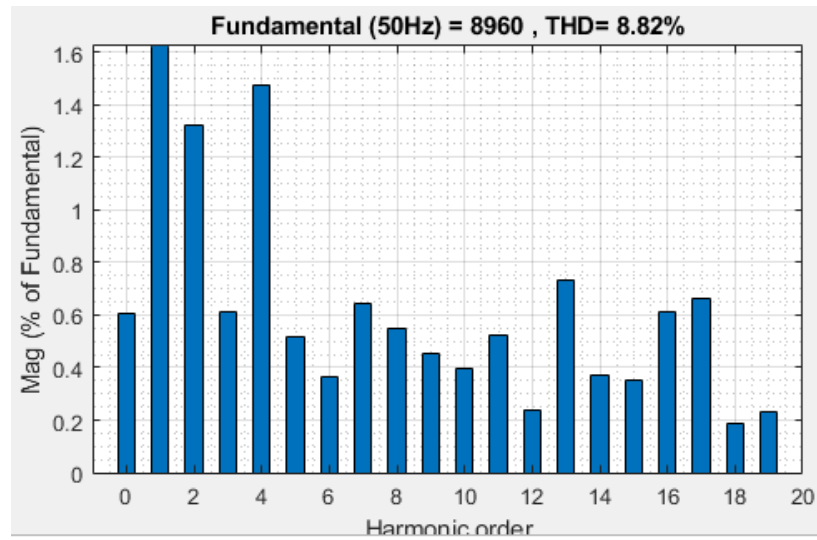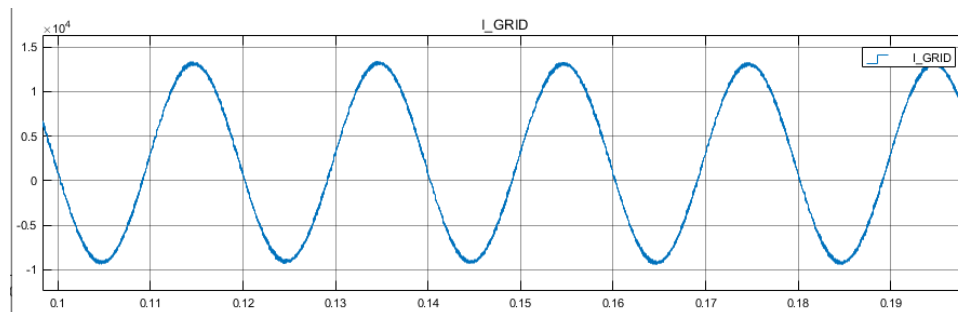

Figure 4. 23: Grid Current after HPF compensation
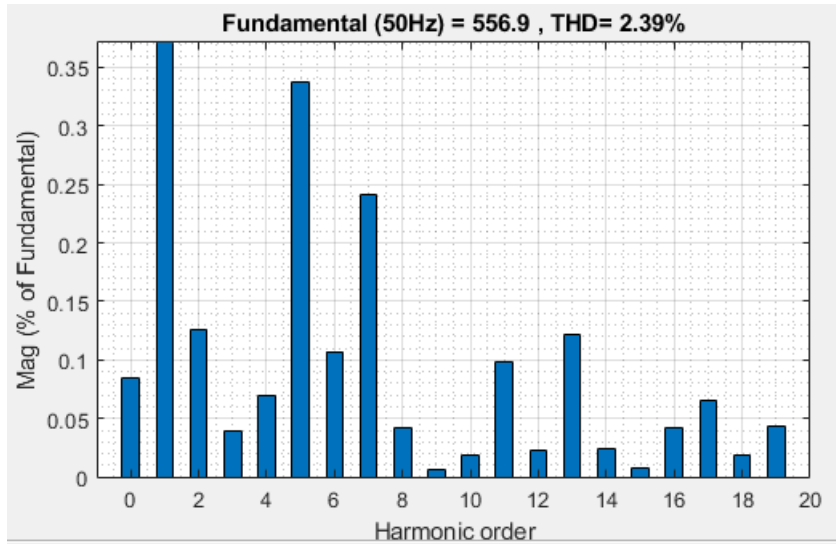
Figure 4. 24: FFT analysis of Grid Current after HPF compensation

Table 4. 6: Individual and THD of Grid current without filter, with hybrid filter and compensation current

Harmonic current order	THD	3rd order	5th order	7th order	11th order	13th order	17th order	19th order
Without filter	29.94	1.24	4.77	3.25	1.51	1.47	4.68	2.83
With Shunt Passive filter	8.82	0.61	0.51	0.64	0.53	0.74	0.66	0.23
With Hybrid filter	2.39	0.04	0.34	0.24	0.10	0.12	0.07	0.04
Compensation current	68.40	1.55	17.33	51.54	2.17	24.09	7.35	12.39

Due to inverter, grid current is distorted (figure 4.6) and inject THD of 29.94% in grid as indicted in figure 4.7. When shunt passive filter is connected to PCC, passive filter draws the harmonic current of order 5th and 7th of fundamental. This improves the nature of the grid current as shown in figure 5.12 and reduces the overall THD from 29.94% to 8.82% as shown in figure 4.13. The 5th and 7th order harmonic source currents are reduced from 4.77% to 0.51% and 3.25% to 0.64% respectively as shown in table 4.6. Before connecting shunt active filter, the THD of the grid current is 8.82% which is beyond IEEE standard. So, shunt active filter is connected in parallel with passive filter at PCC, this reduce the

71

THD to 2.39% as per IEEE standard. The rating of shunt active filter used in this case is 21.96KVA.

Table 4. 7: THD and Individual harmonic distortion of grid current for all scenarios

Harmonic current order	THD	3rd order	5th order	7th order	11th order	13th order	17th order	19th order
Without filter	29.94	1.24	4.77	3.25	1.51	1.47	4.68	2.83
With Shunt Passive filter only	8.82	0.61	0.51	0.64	0.53	0.74	0.66	0.23
With Shunt Active filter only	4.55	0.03	0.81	0.24	0.18	0.01	0.02	0.04
With Hybrid filter	2.39	0.04	0.34	0.24	0.10	0.12	0.07	0.04

The simulation result indicates that the THD of the system is reduced from 29.94% to 8.82% after connecting Shunt Passive filter which is above IEEE-519 standard. When shunt active power filter is connected in parallel with shunt passive filter at the PCC, the overall THD is reduced from 8.82% to 2.39% as per IEEE-519 standard. The shunt active filter used in this case (hybrid power filter) has less rating than case three (active filter only) which is 21.96 KVA.

When Hybrid power filter is used, the THD of grid current is reduced to 2.39% as per IEEE-519 standard. Compared to passive and shunt active power filters, hybrid power filters perform better and also reduce the kVA rating of Shunt active filter.

CHAPTER FIVE

CONCLUSIONS, RECOMMENDATIONS AND SUGGESTIONS FOR FUTURE WORK

5.1 Conclusions

In this thesis, a study of currents harmonics and their consequences on the grid connected PV systems have been discussed. The grid connected PV system is optimally sized and located by using PSO algorithm.

In this thesis 28 bus of Bahir Dar radial distribution feeder R5-02 is considered. Particle swarm optimization algorithm is developed for optimal PV allocation while minimizing real and reactive power loss as well as improving the voltage profile. The result indicates that the active power loss is minimized by 57.97 % whereas the reactive power loss is reduced by 58.49 % which saves 105.95 KW and 154.88 Kvar respectively. From the load flow result of backward forward, the voltage profile of the system is in the desired limit between 0.95p.u and 1.0p.u after PV installation. This confirms that PV system is effective in reducing power losses and improving the voltage profile of the radial distribution network.

Connecting a PV system to the grid needs a power electronics inverter, which injects harmonics into the grid. In this work, a comparative analysis of the performance of passive filter with the hybrid filter for a grid connected PV system is proposed in the optimally sized and located PV system. According to the FFT analysis, the inverter in grid-connected PV system has THD of 29.94%, which is higher than the IEEE standard of 5%. Using MATLAB SIMULINK, the proposed hybrid power filter (shunt passive and shunt active filter) is simulated. The simulation result indicates that the THD of the system is reduced from 29.94% to 8.82% after connecting Shunt Passive filter only at the PCC. The THD of the system is reduced from 29.94% to 4.55% after connecting Shunt active filter only. The THD of the system is reduced from 29.94% to 2.39% after connecting Hybrid power filter as per IEEE-519 standard. Compared to passive and shunt active power filters, hybrid power filters perform better and also reduce the kVA rating of Shunt active filter.

Therefore, it is concluded that Hybrid filters proves to be a cost effective solution for the elimination of harmonics or to improve the performance of the system as compared to active and passive filter used alone.

5.2 Recommendations

To satisfy the demands need of R5-02 distribution customers there must be integration of PV system into the distribution network. Before the integration of PV system into the grid analysis of voltage profile and power loss must be done. This research work identifies the impact of DG to the grid harmonics level and takes measurement by analyzing the harmonics level to how much it affects the system and mitigate the harmonic level by using Hybrid power filter. I highly recommend to Ethiopian Electric Utility (EEU) to apply mitigation of harmonics in grid connected PV system to the feeder of R5-02 since the existing network topology (radial nature) is not designed for futurity of electric demand with the integration of PV system.

This thesis work will help the EEU in reducing both real and reactive power losses in their networks. This reduction in loses will enable them avoid some of the penalties and compensations they incur and hence result to an improvement in their profit margins and their customers as well. The thesis work will also ensure that reduce the THD of grid connected PV system at the PCC to the required limits. This will enable the EEU and EEP to ensure proper operation of equipment and a longer equipment life span by keeping values of harmonic distortion in acceptable limit on a distribution system. As a result, this makes the companies more economical and reliable in operation.

5.3 Future Works

The presented work can be extended in other following related areas:

- ❖ To verify diversified models using designed filter to mitigate harmonics
- ❖ Study and implementation of various control techniques of shunt active filters helps to mitigate power quality issues faced in electrical utilities. Also, soft computing techniques such as the fuzzy logic control can be further researched and implemented.
- ❖ To implement the control strategy using Artificial Intelligence (AI) techniques.

REFERENCES

[1] A. Agrawal and D. K. Singh, Harmonic Impact of Grid Connected Photovoltaic, 3rd ed., Int. Conf. Converg. Technol, 2018.

[2] Krischonme Bhumkittipich and Weerachai Phuangpornpitak, "Optimal Placement and Sizing of Distributed Generation for Power Loss Reduction using Particle Swarm Optimization," *10th Eco-Energy and Materials Science and Engineering,* p. 307 – 317, 2013.

[3] J Sreedevi, Ashwin N, M Naini Raju, A Study on Grid Connected PV system, india, 2016, pp. 0-5.

[4] D. Committee, I. Power, and E. Society, IEEE Recommended Practice and Requirements for Harmonic Control in Electric Power Systems IEEE Power and Energy Society, 2014.

[5] A. J. Mehta and K. Mokariya, Harmonics in Power System and its Mitigation, 2012, pp. 9-12.

[6] H. A. Kazem, Harmonic mitigation techniques applied to power distribution, 2013.

[7] M. S. a. M. R. Rahul, "Optimal placing and sizing of DG in a distribution system for voltage stability improvement," *IEEE,International Conf. Electr. Electron. Optim. Tech. ICEEOT 2016,* p. 1469–1475, 2016.

[8] Mounika Lakshmi Prasanna K, Amit Jain and James Ranjith Kumar R, "Particle Swarm Optimization Application for Optimal Location of Multiple Distributed Generators in Power Distribution Network," *J Electr Electron Syst, an open access journal,* vol. 6, no. 4, 2017.

[9] M. Tali, A. Obbadi, A. Elfajri, and Y. Errami, "Passive filter for harmonics mitigation in standalone PV system for non linear load," p. 499–504, 2014.

[10] Xu Renzhong, Xia Lie, Zhang Junjun, and Ding Jie, "Design and Research on the LCL Filter in Three-Phase PV Grid-Connected Inverters," *International Journal of Computer and Electrical Engineering,* vol. 05, no. 03, June 2013.

[11] B. H. Yong and V. K. Ramachandaramurthy, "Double tuned filter design for harmonic mitigation in grid connected solar PV," *Conf. Proceeding - 2014 IEEE Int. Conf. Power Energy, PECon 2014,* p. 293–297, 2014.

[12] Suleyman Adak, Hasan Cangi and Ahmet Serdar Yilmaz, "Design of an LLCL type filter for stand-alone PV systems' harmonics," *Journal of Energy Systems,* vol. 3, no. 1, 2019.

[13] M. Adel, S. Zaid, and O. Mahgoub, "Improved active power filter performance based on an indirect current control technique," *Journal of Power Electronics,* vol. 11, no. 6, pp. 931-937, 2011.

[14] M. J. M. A. Rasul, H. V Khang, and M. Kolhe, "Harmonic Mitigation of a Grid-connected Photovoltaic System using Shunt Active Filter".

[15] K. D. Priyanka and P. Suresh, "Mitigation of Harmonics in Grid Connected Hybrid Renewable Energy Sources at The Distribution Level," vol. 7, no. 2, p. 1692–1698, 2019.

[16] T. Belgore, "Control Techniques for Shunt Active Power Filters," vol. 9, no. 09, p. 1054–1059, 2020.

[17] R. Baharom, I. M. Yassin, and M. N. Hidayat, "ctive power filter with hysteresis current control loop using rectifier boost technique," vol. 11, no. 3, p. 1117–1122, 2020.

[18] E. Ciprés, "Analysis of The Implementation of a Photovoltaic Plant in Distribution," February, 2011.

[19] B. Tesfaye, "Improved Sustainable Power Supply for Dagahabur and Kebridahar Town of Somalia Region in Ethiopia," 2011.

[20] Gudimetla.B, Katriraei.F Aquero.J.R and Enslin.J.H.R, "Integration of Micro-Scale Photovoltaic Distributed Generation on Power Distribution Systems," *Dynamic Analysis,* no. IEEE Transmission and Distribution Conference and Exposition, 7 may 2012.

[21] M. R. Patel, Wind and Solar Power Systems, New York, 1999.

[22] J. B. Gupta, "A Course In Power Systems," p. 1600, 2009.

[23] M. E. N. O. F. En, "Photovoltaics: Basic Principles and Components," 1997.

[24] A. Jayavarma and T. Joseph, "Optimal Placement of Solar PV in Distribution System using Particle Swarm Optimization," p. 329–337, 2013.

[25] W. Krueasuk and W. Ongsakul, "Optimal Placement of Distributed Generation Using Particle Swarm Optimization," *Australian Universities Power Engineering Conference,* 10-13 Dec 2006.

[26] R. Poli, "Analysis of the publications on the applications of particle swarm optimisation," *Journal of Artificial Evolution and Applications,* 2008.

[27] P. G. Student, P. College, and A. Pradesh, "Mitigation of Current Harmonics in A Solar Hybrid System By Using Hybrid Filter," p. 526–531, 2016.

[28] R. Gokarapu, "Determination of Harmonics for Modeling Integration of Solar Generation to The Electric Grid," 2011.

[29] Z. Hameed, A. Yousaf, M. Rafay, and K. Sial, "Harmonics in Electrical Power Systems and how to remove them by using filters in ETAP," february 2016.

[30] D. M. Tobnaghi, "A Review on Impacts of Grid-Connected PV System on Distribution Network," *International Journal of Electrical, Computer, Energetic, Electronic and Communication Engg,* vol. 10, no. 1, 2016.

[31] S. Rafiei, "Application of distributed generation sources for Micro-Grid power quality enhancement," 2014.

[32] B. S. Kumar, "MITIGATION OF LOWER ORDER HARMONICS IN A GRID CONNECTED THREE PHASE PV INVERTER," 2015.

[33] Patricio Santis, Doris Sáez, Roberto Cárdenas, Alfredo Núñez, "Paretobased modulated model predictive control strategy for power converter applications," no. Electr. Power Syst. Res. (171) , pp. 158-174, 2019.

[34] S.M. Tayebi, I. Batarseh, "Mitigation of current distortion in a three-phase microinverter with phase skipping using a synchronous sampling DC-link voltage control," no. IEEE Trans. Ind. Electron. 65 (5), pp. 3910-3920, 2018.

[35] A. Nazemi Babadi, O. Salari, M.J. Mojibian, M.T. Bina, "Modified multilevel inverters with reduced structures based on packed U-cell," no. IEEE J. Emerg. Sel. Top. Power Electron. 6 (2) , pp. 874-887, 2018.

[36] C. Han, "Power system dynamic voltage management with advanced STATCOM and energy storage system," 2006.

[37] D. Bhadra, R. K. Meena, and E. Engineering, "POWER QUALITY IMPROVEMENT BY HARMONIC REDUCTION USING THREE PHASE SHUNT ACTIVE POWER FILTER WITH p-q & d-q CURRENT CONTROL STRATEGY".

[38] GagandeepKaur and Dr. Ritula Thakur, "DESIGN OF SHUNT PASSIVE FILTER FOR HARMONIC MITIGATION," *International Journal of Current Research,* vol. 8, no. 06, pp. 33307-33312, June 2016.

[39] H. Akagi, Edson.H. Watanabe and M. Aredes, "Instantaneous Power Theory and applications to power conditioning," *IEEE Press Chapter 3- 4,* pp. 19-107, 2007.

[40] N.Vanajakshi, G.Nageswara Rao, "A Three Phase Shunt Active Power Filter For Harmonics Reduction," *International Research Journal of Engineering and Technology (IRJET) e-ISSN: 2395-0056,* vol. 02, no. 09, Dec-2015.

[41] M. Kmail, "Investigation Of Shunt Active Power Filter For Power Quality Improvement," 2012.

[42] J. M. Sadeq, "Comparative Study Of Passive, Series And Shunt Active Power Filters With Hybrid Filters On Nonlinear Loads," 2014.

[43] Kumaresan, S._ Habeebullah Sait, H. , "Design and control of shunt active power filter for power," *Journal for Control Measurement Electronics Computing and Communications ,* vol. 61, no. 3, 2020-jul 02.

[44] M. Aredes, E. H. Watanabe, "New Control Algorithms for Series and Shunt Three Phase Four-Wire Active Power Filters," *IEEE Trans. Power Delivery,* vol. 10, no. 03, pp. 1649-1656, July-1995.

[45] A. Zouidi, F. Fnaiech and K. Al-Haddad, "Voltage source Inverter Based three-phase shunt active Power Filter: Topology, Modeling and Control Strategies," *2006 IEEE International Symposium on Industrial Electronics, Montreal, Que.,* pp. 785-790, 2006.

[46] D. Detjen, J. Jaeobs, R.W.De Doneker and H.G. Mall, "A New Hybrid Filter to Dampen Resonances and Compensate Harmonic Currents in Industrial Power Systems with Power Factor Correction Equipment," *IEEE Transactions on Power Electronics,* vol. 16, no. 6, pp. 821-827, Nov-2001.

[47] L. Hac, "Elimination of Harmonics Using Active Power Filter Based on DQ Reference Frame Theory".

[48] C. S. e. al, "Analysis, design and digital implementation of a SAPF with different schemes of reference current generation," *Power Electron IET,* 2013.

[49] M. V. Elango Sundaram, "On design and implementation of three phase three level shunt active power filter for harmonic reduction using synchronous reference frame theory," *Electrical Power and Energy Systems,* pp. 40-46, 2016.

[50] E. Hossain, MATLAB and Simulink Crash Course for Engineers.

[51] Sathiyanarayanan T. and S. Mishra, "Synchronous Reference Frame Theory based Model Predictive Control for Grid Connected Photovoltaic Systems," *Department*

of Electrical Engineering, Indian Institute of Technology Delhi-110016, p. 766–771, 2016.

[52] S. A. V. M. Vahedi H, "Review and simulation of fxed and adaptive hysteresis current control considering switching loss and high frequency harmonics," *Adv Power Electron,* pp. 1-6, 2011.

[53] S. Chandrasiri, "Temperature effect on solar photovoltaic power generation," no. January 2017, 2019.

[54] N. Farahiah, B. Ibrahim, Z. Bin, A. Bakar, W. Suhaifiza, and B. W. Ibrahim, "The Feasibility Study of Solar PV Lighting," *IEEE,* p. 92–96, 2016.

[55] H. A. Kefale, E. M. Getie, and K. G. Eshetie, "Optimal Design of Grid-Connected Solar Photovoltaic System Using Selective Particle Swarm Optimization," *International Journal of Photoenergy,* vol. 2021, 2021.

[56] J. A. M. Rupa and S. Ganesh, "Power Flow Analysis for Radial Distribution System Using Backward / Forward Sweep Method," vol. 8, no. 10, p. 1628–1632, 2014.

[57] Ghatak, U., Mukherjee, V, "A fast and efficient load flow technique for unbalanced distribution system," *Int. J. Electr. Power Energy Syst ,* vol. 84, pp. 99-110, 2017.

[58] S. Devi and M. Geethanjali, "Optimal location and sizing determination of Optimal location and sizing determination of algorithm," *Int. J. Electr. Power Energy Syst,* vol. 62, p. 562–570, 2014.

[59] C. Shrivastava, M. Gupta, and A. Koshti, "Review of Forward & Backward Sweep Method for Load Flow Analysis of Radial Distribution System," p. 5595–5599, 2015.

[60] S. Sunisith and K. Meena, "Backward / Forward Sweep Based Distribution Load Flow Method," vol. 5, no. 9, p. 1539–1544, 2014.

[61] C. L. Wadhwa, Electrical Power system, sixth ed., New Age International Publication, 2010.

[62] H. Sadat, Power system analyses, TMH Publication, 2002.

[63] Advanced power converters for universal and flexible power management in future electricity network, University of Notthingham, Aalborg University, 2007.

[64] O. G. O. A. E. S. E. Alroza Khaligh, "ENERGY HARVESTING, solar, wind, and ocean energy conversion systems.," *Energy, Power Electronics, and Machines Series,,* 2010.

[65] M. H. Rashid, Power Electronics circuits, Devices and Applications, Third ed.

[66] M. I. a. D. S. Muhammad Rusli, "SINGLE TUNED HARMONIC FILTER DESIGN AS TOTAL HARMONIC DISTORTION (THD) COMPENSATOR," *23rdInternational Conference on Electricity Distribution,* June 2015.

[67] Y.-S. C. &. H. Cha, "Single-tuned Passive Harmonic Filter Design Considering Variances of Tuning and Quality Factor," *Journal of International Council on Electrical Engineering,* vol. 1, no. 1, p. 7~13, 2011.

[68] M. T. Shah, D. Nagotha, "Response Analysis of Shunt Active Power Filter Under Various Line and Load Side Conditions," *Book chapter in Advances in Intelligent Systems Research, Atlantis Press,* vol. 137, pp. 395-403, 2016.

[69] A. J.-P. G. F. K. a. L. R. Chaoui, "On the design of shunt active filter for improving power quality.," *IEEE International Symposium on Industrial Electronics,* pp. 31-37, 2008.

[70] K. F, "Parameters estimation of Shunt Active Filter for Power quality improvement," *5th IEEE International Conference on Power Engineering and Optimization,* pp. 306-311, 2011.

[71] S. V. Patel and M. T. Shah, "Three-phase front end converters and current control techniques for unity power factor," *2013 Nirma University International Conference on Engineering (NUiCONE),* pp. 1-5, 2013.

[72] J. K. Charles, System Loss Reduction and Voltage Profile Improvement, 2011.

[73] D. Pandey and J. S. Bhadoriya, "Optimal Placement & Sizing Of Distributed Generation (DG) To Minimize Active Power Loss Using Particle Swarm Optimization (PSO)," vol. 3, no. 7, p. 246–254, 2014.

APPENDICES

APPENDIX A: Solar module datasheet

Characteristics	Value
Manufacturer	TATA solar power
Peak power @ standard test condition (STC) (W)	300
Voltage @peak power (V)	36.6
Current @ peak power (A)	8.2
Open circuit voltage (V)	44.8
Short circuit current (A)	8.71
Power tolerance(W)	0 ~ +5
Efficiency (%)	15.1
module efficiency (%/°C)	0.06 ± 0.01
Temperature coefficient of Pmax (%/°C)	0.4048
Temperature coefficient of Voc (%/°C)	0.2931
Temperature coefficient of Isc (%/°C)	0.0442
Nominal operating temperature *(NOCT)* (°C)	42±2

APPENDIX B: Inverter datasheet

Characteristics	Value
Manufacturer	Bonfiglioli
Input data DC	
Maximum DC power	280KW
Maximum DC Voltage (V)	900 V
Maximum DC Current (A)	600 A
MPPT Voltage range	425-975 V
Output data AC	
Maximum AC power	250 KW
Output AC voltage range(V)	270-330 V
Maximum AC current (A)	540 A
Efficiency (%)	98.3 %

APPENDIX C: Line and Load data of the feeder R5-02

Sending node	Receiving node	Conductor type	Length (Km)	Resistance (Ω)	Reactance (Ω)	Receiving end load (KW)	Receiving end load (KVAr)
1	2	AAAC-200	0.001	0.0001757	0.000273	0	0
		AAAC-200	0.602	0.1057714	0.164346		
		UG-Cable-300	0.214	0.0168846	0.0218066		
		AAAC-200	3.082	0.5415074	0.841386		
		UG-Cable-300	0.148	0.0116772	0.0150812		
		AAAC-200	2.271	0.3990147	0.619983		
		UG-Cable-300	0.192	0.0151488	0.0195648		
		AAAC-200	1.184	0.2080288	0.323232		
		UG-Cable-300	0.05	0.003945	0.005095		
		Total	**7.744**	**1.3021536**	**2.0107676**		
2	3	UG-Cable-300	0.05	0.003945	0.005095	22.6	10.69
		AAAC-150	0.211	0.0463145	0.0590378		
		Total	**0.2611**	**0.0502595**	**0.0641328**		
3	4	AAAC-150	0.195	0.0428025	0.054561	0	0
		UG-Cable-300	0.201	0.0158589	0.0204819		
		AAAC-150	0.048	0.010536	0.0134304		
		Total	**0.444**	**0.0691974**	**0.0884733**		
4	5	AAC-50	0.246	0.16728	0.089052	569.52	269.33
4	6	AAAC-150	0.182	0.039949	0.0509236	0	0
6	7	AAAC-150	0.265	0.0581675	0.074147	0	0
		AAAC-150	0.067	0.0147065	0.0187466		
		Total	**0.332**	**0.072874**	**0.0928936**		
7	8	AAC-25	0.194	0.259572	0.07372	361.6	171
7	9	AAAC-150	0.056	0.012292	0.0156688	45.2	21.38
9	10	AAAC-150	0.26	0.05707	0.072748	90.4	42.75
3	11	AAC-95	0.539	0.182721	0.181643	284.76	134.66
11	12	AAC-95	0.21	0.07119	0.07077	284.76	134.66
12	13	AAC-95	0.09	0.03051	0.03033	90.4	42.75

6	14	AAC-50	0.084	0.05712	0.030408	180.8	85.5
14	15	AAC-50	0.023	0.01564	0.008326	659.92	312.08
15	16	AAC-50	0.123	0.08364	0.044526	0	0
16	17	AAC-50	0.115	0.0782	0.04163	452	213.75
16	18	AAC-50	0.255	0.1734	0.09231	180.8	85.5
18	19	AAC-50	0.273	0.18564	0.098826	180.8	85.5
19	20	AAC-50	0.332	0.22576	0.120184	180.8	85.5
20	21	AAC-50	0.149	0.10132	0.053938	0	0
21	22	AAC-50	0.144	0.09792	0.052128	22.6	10.69
21	23	AAC-50	0.328	0.22304	0.118736	90.4	42.75
23	24	AAC-50	0.097	0.06596	0.035114	0	0
24	25	AAC-50	0.092	0.06256	0.033304	180.8	85.5
24	26	AAC-50	0.673	0.45764	0.243626	180.8	85.5
26	27	AAC-50	0.1	0.068	0.0362	180.8	85.5
27	28	AAC-50	0.296	0.20128	0.107152	180.8	85.5

APPENDIX D: Simulation Code for Load Flow

```
Function[finalres]=load_flow_process_basecase(nbus,data_pas
s_to_loadflow)

source_num=[1];
[LINEDATA]=linedata_radial_bus(nbus);
BUSDATA=busdata_radial_bus(nbus);
baseKV=15;baseMVA=100;
PBASE=baseMVA*1000;VBASE=(baseKV^2)/baseMVA;
busdata_value=BUSDATA;linedata_value=LINEDATA;

linedata_value(:,4:5)=linedata_value(:,4:5)/VBASE;
resistance_val=linedata_value(:,4);
reactance_val=linedata_value(:,5);
actual_imped=complex(resistance_val,reactance_val);
busdata_value(:,2:3)=(busdata_value(:,2:3)/PBASE);
imped_value=actual_imped;
[bibc_matrix]=bibc_gen(linedata_value,busdata_value);

bibc_matrix(source_num,:)=[];
bibc_matrix(:,source_num)=[];

final_bibc_matrix=bibc_matrix';
```

```matlab
final_bcbv_matrix=final_bibc_matrix'*diag(actual_imped);
final_dlf_matrix=final_bcbv_matrix*final_bibc_matrix;
complex_load_d=complex(busdata_value(:,2),busdata_value(:,3
));% complex power load
complex_load_g=zeros(size(busdata_value,1),1);
final_load_matrix=(complex_load_d-complex_load_g);
final_load_matrix(length(source_num))=[];
initial_volt_value=ones(size(busdata_value,1)-
length(source_num),1);% initial bus voltage
voltage_drop_value=initial_volt_value;
max_iter=100;
for ind_lop=1:max_iter
    %backward sweep

inject_current_data=conj(final_load_matrix./voltage_drop_va
lue); % injected current at each bus
    IB=final_bibc_matrix*inject_current_data; %get the
cumulative injected current flowing through each branch
    old_volt=voltage_drop_value;
    volt_drop_each=final_dlf_matrix*inject_current_data;
%voltage drops along each branch.
    voltage_drop_value=initial_volt_value-volt_drop_each;
    old_volt1=(old_volt);
    new_volt=(voltage_drop_value);
    error_volt_tolr=max(abs(old_volt1-new_volt));
end
final_volt_data=[ones(length(source_num),1);voltage_drop_va
lue];
locvoltm=find(final_volt_data>1);
final_volt_data(locvoltm)=1;
from_node=linedata_value(:,2);
to_node=linedata_value(:,3);
for ind=1:length(from_node)
    volt_diff_value(ind,:)=final_volt_data(from_node(ind))-
final_volt_data(to_node(ind));
end
volt_diff_value1=abs(volt_diff_value);
ploss=((volt_diff_value1.^2).*resistance_val)./(abs(imped_v
alue).*abs(imped_value))*10^5; % Each Line Loss in kWs
loc1=find(~(isnan(ploss)));
qloss=((volt_diff_value1.^2).*reactance_val)./(abs(imped_va
lue).*abs(imped_value))*10^5; % Each Line Loss in kVAr
loc2=find(~(isnan(qloss)));
total_power_lossp=sum(ploss(loc1));
total_power_lossq=sum(qloss(loc2));
finalvoltage=real(final_volt_data);
finalres{1}=total_power_lossp;
```

```
finalres{2}=total_power_lossp;
finalres{3}=total_power_lossq;
finalres{4}=finalvoltage;
finalres{5}=ploss;
```

APPENDIX E: Simulation Code for Optimal size and location of PV using PSO

```
clc
clear all;
close all;
warning off;

disp('****************************************************
********************');
disp('OPTIMAL PLACEMENT OF DISTREIBUTED GENERATION FOR LOSS
REDUCTION USING PSO');
disp('****************************************************
********************');

pop=input('Enter the Population Value:--');
iter=input('Enter the Iteration Value:--');
DG=input('Specify Number of DG,1 or 2 or 3 or 4:--');
bus_no=input('Enter the IEEE Bus System for Testing,25 or
28:--');
%% DG size minimum and maximum value
no_of_DG=DG; %no of DG placement
DG_SIZE_MIN=10;
DG_SIZE_MAX=2000;
% voltage minimum and maximum
voltage_minimum=0.95;
voltage_maximum=1.05;
current_maximum=2000;
nbus=bus_no;
no_of_int_pop=pop; % number of initial population
no_of_iter=iter; % number of iteration

data_pass_to_loadflow{2}=voltage_minimum;
data_pass_to_loadflow{3}=voltage_maximum;
data_pass_to_loadflow{4}=current_maximum;
data_pass_to_loadflow{12}=no_of_DG;
%% apply load flow base case
[objective_result]=load_flow_process_basecase(nbus,data_pas
s_to_loadflow);
%Display  Power Loss
%POWER_LOSS_BASE_CASE=objective_result{1};
%%
```

```matlab
%Display Power Loss in Real and Reactive value
ACTIVE_POWER_LOSS_BASE_CASE=objective_result{1};
REACTIVE_POWER_LOSS_BASE_CASE=objective_result{3};
VOLTAGE_BASE_CASE=objective_result{4};
BASE_CASE_RESULT=table(ACTIVE_POWER_LOSS_BASE_CASE,REACTIVE
_POWER_LOSS_BASE_CASE)
pause(3);
%%  Only DG
for km=2:nbus
min_val1=km;    % lower limit
max_val1=km;  % upper limit
min_val2=DG_SIZE_MIN;    % lower limit
max_val2=DG_SIZE_MAX;  % upper limit
data_pass_to_loadflow{12}=1;
no_in_val=1;

%% PSO algorithm process
[data_final_pso,final_fit_pso]=PSO_PROCESS_dgplace(nbus,no_
of_int_pop,...
no_of_iter,min_val1,max_val1,min_val2,max_val2,...

no_in_val*2,data_pass_to_loadflow);
FINAL_DG_loc=data_final_pso;
[objective_result]=load_flow_process_withdg(nbus,...

FINAL_DG_loc,data_pass_to_loadflow);
POWER_LOSS_p=objective_result{2};
POWER_LOSS_q=objective_result{3};
BUS_NUMBER(km-1,1)=FINAL_DG_loc(1);
DG_SIZE_MW(km-1,1)=FINAL_DG_loc(2)/1000;
Ploss_KW(km-1,1)=POWER_LOSS_p;
Qloss_KVar(km-1,1)=POWER_LOSS_q;
end
if(nbus==25)
RESULT_OF_25_BUS_SYSTEM=table(BUS_NUMBER,DG_SIZE_MW,Ploss_K
W,Qloss_KVar)
else
RESULT_OF_28_BUS_SYSTEM=table(BUS_NUMBER,DG_SIZE_MW,Ploss_K
W,Qloss_KVar)
end
figure,plot(BUS_NUMBER,DG_SIZE_MW,'m-^','linewidth',2);
xlabel('Bus Number');ylabel('DG Size MW');grid on;
% title('Suitable DG size of a 64-bus test system');
% title(['PSO Suitable DG size for IEEE BUS-28'
num2str(bus)]);
data_pass_to_loadflow{12}=no_of_DG;
%%  Only DG placement
```

```matlab
min_val1=2;    % lower limit
max_val1=nbus;   % upper limit
min_val2=DG_SIZE_MIN;    % lower limit
max_val2=DG_SIZE_MAX;   % upper limit
no_in_val=no_of_DG;
%% PSO algorithm process
[data_final_pso,final_fit_pso]=PSO_PROCESS_dgplace(nbus,no_
of_int_pop,.
..
no_of_iter,min_val1,max_val1,min_val2,max_val2,...

no_in_val*2,data_pass_to_loadflow);
FINAL_DG_loc=data_final_pso;
DG_LOCATION=FINAL_DG_loc(1:no_of_DG)
DG_SIZE_Kw=(FINAL_DG_loc(no_of_DG+1:end))
[objective_result]=load_flow_process_withdg(nbus,...

FINAL_DG_loc,data_pass_to_loadflow);
POWER_LOSS_p=objective_result{2};
POWER_LOSS_q=objective_result{3};
LINE_LOSS_p=objective_result{5};
VOLTAGE_WITH_DG=objective_result{4};
%% plot loss and voltage graph
 % ALG_NAME='PSO';
figure,bar(1:length(LINE_LOSS_p),LINE_LOSS_p,'c');
xlabel('Line Number');ylabel('Real Power Loss');grid on;
title('Power Loss of a 28-bus test system');
pause(3);
figure,plot(1:length(VOLTAGE_BASE_CASE),VOLTAGE_BASE_CASE,'
r-','linewidth',2);
hold on;plot(1:length(VOLTAGE_WITH_DG),VOLTAGE_WITH_DG,'b-
','linewidth',2);
xlabel('Bus Number');ylabel('Bus Voltage');grid on;
title('Voltage Profile-Particle Swarm Optimization');
legend('Basecase Without
DG'),['With',num2str(no_of_DG),'DG'];
pause(3);

figure,plot(1:length(final_fit_pso),final_fit_pso,'k-
s','linewidth',2);
xlabel('Iteration');ylabel('Fitness');grid on;
title('Convergence Graph');
pause(3);

EFFICIENCY=((ACTIVE_POWER_LOSS_BASE_CASE-
min(Ploss_KW))/ACTIVE_POWER_LOSS_BASE_CASE)*100;
RESULT=table(DG_LOCATION,DG_SIZE_Kw,EFFICIENCY)
```